β4 Integrin signaling induces expansion of prostate tumor progenitors

Toshiaki Yoshioka, … , Charles L. Sawyers, Filippo G. Giancotti

Research Article

The contextual signals that regulate the expansion of prostate tumor progenitor cells are poorly defined. We found that a significant fraction of advanced human prostate cancers and castration-resistant metastases express high levels of the β4 integrin, which binds to laminin-5. Targeted deletion of the signaling domain of β4 inhibited prostate tumor growth and progression in response to loss of p53 and Rb function in a mouse model of prostate cancer (PB-*TAg* mice). Additionally, it suppressed *Pten* loss-driven prostate tumorigenesis in tissue recombination experiments. We traced this defect back to an inability of signaling-defective β4 to sustain self-renewal of putative cancer stem cells in vitro and proliferation of transit-amplifying cells in vivo. Mechanistic studies indicated that mutant β4 fails to promote transactivation of ErbB2 and c-Met in prostate tumor progenitor cells and human cancer cell lines. Pharmacological inhibition of ErbB2 and c-Met reduced the ability of prostate tumor progenitor cells to undergo self-renewal in vitro. Finally, we found that β4 is often coexpressed with c-Met and ErbB2 in human prostate cancers and that combined pharmacological inhibition of these receptor tyrosine kinases exerts antitumor activity in a mouse xenograft model. These findings indicate that the β4 integrin promotes prostate tumorigenesis by amplifying ErbB2 and c-Met signaling in tumor progenitor cells.

Find the latest version:

https://jci.me/60720/pdf

β4 Integrin signaling induces expansion of prostate tumor progenitors

Toshiaki Yoshioka,[1,2] Javier Otero,[1] Yu Chen,[3,4] Young-Mi Kim,[1] Jason A. Koutcher,[5]
Jaya Satagopan,[6] Victor Reuter,[7] Brett Carver,[3,4] Elisa de Stanchina,[8] Katsuhiko Enomoto,[2]
Norman M. Greenberg,[9] Peter T. Scardino,[10] Howard I. Scher,[4]
Charles L. Sawyers,[3] and Filippo G. Giancotti[1]

[1]Cell Biology Program, Sloan-Kettering Institute for Cancer Research, Memorial Sloan-Kettering Cancer Center (MSKCC), New York, New York, USA.
[2]Departments of Molecular Pathology and Tumor Pathology, Akita University Graduate School of Medicine, Akita, Japan.
[3]Human Oncology and Pathogenesis Program, [4]Department of Medicine, [5]Department of Medical Physics, [6]Department of Epidemiology and Biostatistics,
and [7]Department of Pathology, Memorial Hospital, MSKCC, New York, New York, USA. [8]Antitumor Assessment Core, MSKCC, New York, New York, USA.
[9]Division of Clinical Research, Fred Hutchinson Cancer Research Center, Seattle, Washington, USA.
[10]Department of Surgery, Memorial Hospital, MSKCC, New York, New York, USA.

The contextual signals that regulate the expansion of prostate tumor progenitor cells are poorly defined. We found that a significant fraction of advanced human prostate cancers and castration-resistant metastases express high levels of the β4 integrin, which binds to laminin-5. Targeted deletion of the signaling domain of β4 inhibited prostate tumor growth and progression in response to loss of p53 and Rb function in a mouse model of prostate cancer (PB-*TAg* mice). Additionally, it suppressed *Pten* loss-driven prostate tumorigenesis in tissue recombination experiments. We traced this defect back to an inability of signaling-defective β4 to sustain self-renewal of putative cancer stem cells in vitro and proliferation of transit-amplifying cells in vivo. Mechanistic studies indicated that mutant β4 fails to promote transactivation of ErbB2 and c-Met in prostate tumor progenitor cells and human cancer cell lines. Pharmacological inhibition of ErbB2 and c-Met reduced the ability of prostate tumor progenitor cells to undergo self-renewal in vitro. Finally, we found that β4 is often coexpressed with c-Met and ErbB2 in human prostate cancers and that combined pharmacological inhibition of these receptor tyrosine kinases exerts antitumor activity in a mouse xenograft model. These findings indicate that the β4 integrin promotes prostate tumorigenesis by amplifying ErbB2 and c-Met signaling in tumor progenitor cells.

Introduction

Prostate cancer, the most common noncutaneous malignancy diagnosed in men, progresses from carcinoma in situ, termed prostatic intraepithelial neoplasia (PIN), to invasive and metastatic cancer, suggesting that multiple genetic and epigenetic lesions contribute to its development. Although significant progress has been made toward early detection and treatment, once it has become metastatic, prostate cancer cannot be cured (1, 2). Patterns of allelic loss in human prostate cancer specimens and reverse genetic approaches in the mouse have suggested that loss of function mutations in *NKX3.1*, *PTEN*, *RB*, and *P53* and overexpression of *MYC* promote prostate cancer progression (3). Studies using outlier gene expression analysis have revealed that oncogenic gene fusions juxtaposing 5′ androgen-controlled regulatory elements to Ets transcription factors, such as *ERG*, are prevalent in human prostate cancer (4). In addition, integrative genomic profiling of a large data set (*n* = 218) has provided evidence that allelic losses and gains disrupting the Rb and p53 signaling networks and activating the PI-3K and the Ras/Raf signaling pathways are also common in primary prostate cancers, whereas amplifications and mutations of the androgen receptor (AR) are restricted to metastatic lesions (5).

Increasing evidence suggests that oncogenic mutations exert their action by transforming adult stem cells or transit-amplifying cells into neoplastic progenitor cells, thereby spurring the development of cancers that consist of tumor progenitor cells as well as aberrantly differentiated cells (6–8). The tumor progenitor cells are operationally defined by their ability to undergo self-renewal in vitro and to initiate secondary tumors upon xenotransplantation in mice. Furthermore, these cells are relatively resistant to both chemotherapy and oncogene-targeted therapies, suggesting that their expansion might drive most of the relapses observed in the clinic (9). In spite of significant recent progress, the contextual cues that regulate normal stem cells and their rapidly proliferating immediate progeny, the transit-amplifying cells, remain unknown.

Prostatic glands are composed of a continuous layer of columnar secretory cells resting on a layer comprising basal cells and scattered neuroendocrine cells, both of which are in direct contact with a basement membrane (10). Prospective identification and lineage-tracing experiments have led to the identification of potential stem cells in both the basal and the luminal compartments of the mouse (11, 12). Since human prostate cancers are characterized by a loss of normal basal cells, and by an expansion of cells that morphologically and biochemically resemble luminal cells, it has been hypothesized that these tumors arise from neoplastic conversion of a luminal progenitor (13, 14). In agreement with this hypothesis, lineage-tracing experiments have suggested that the luminal layer of the mouse prostate contains Nkx3-1–positive bipotential progenitors, which can be directly converted into neoplastic cells by inactivation of *Pten* (12). Basal cells are seemingly resistant to direct transformation, unless loss of Pten induces them to differentiate into transformation-competent luminal cells (15). In contrast, the luminal compartment of the human prostate is refractory to transformation in

Table 1
COPA of *ITGB4* and *ERG* in prostate cancer data sets

ITGB4			ERG			Data set	Refs.
Score	Rank	%	Score	Rank	%		
26.6	1%	90	1.8	8	75	Welsh	93
25.5	4%	75	39.3	3	95	Magee	94
7.4	10%	75	3.6	10	75	Luo	95
5.5	1%	95	1.2	10	75	Nanni	96
4.4	3%	95	1.7	1	75	LaTulippe	34
3.0	7%	95	4.2	1	75	Varambally	97
2.8	8%	90	n.d.	n.d.	n.d.	True	98
2.0	10%	75	5.8	6	95	Singh	35
2.0	8%	90	2.3	1	75	Bittner[A]	
1.1	7%	75	4.0	1	75	Vanaja	63
1.0	4%	75	6.6	1	90	Wallace	61

COPA identified *ITGB4* as markedly overexpressed in a subset of tumor samples in 11 out of 16 data sets available from Oncomine (gene rank, top 10%; fold change, >2; $P < 1 \times 10^{-4}$). Using the same statistical filters, *ITGB4* exhibited a COPA score comparable to or higher than that of *ERG* in several data sets. n.d., not determined. [A]GEO accesion no. GSE2109.

vitro by simultaneous introduction of activated Akt, ERG, and AR, whereas the basal cells contain bipotential progenitors that can be transformed by this combination of oncogenes (16, 17).

The signaling pathways that govern the expansion of prostate tumor progenitor cells are incompletely understood. Adult stem cells undergo self-renewal and differentiation in response to contextual cues originating from the specialized microenvironment ("niche") in which they reside (18). Because of its ability to support cell adhesion and signaling by binding to integrins and its presence in many stem cell niches, the basement membrane appears to be especially well-suited to regulate stem cell behavior (19). Among laminin-binding integrins, the α6 subunit–containing integrins, α6β1 and α6β4, are excellent candidates to mediate the effects of basement membranes on stem cells. In fact, the α6 subunit (CD49f) has been broadly used for enrichment of adult stem cells and tumor progenitor cells from many tissues, including the mammary gland (20) and the prostate gland (11, 16). Moreover, a recent study has shown that silencing of α6 reduces the self-renewal and tumor formation capacity of glioblastoma stem cells (21).

The α6β4 integrin (referred to herein as β4 integrin because β4 pairs only with α6) binds to laminin-5, a major component of the basement membrane of the prostate (22), and is characterized by a signaling mechanism that is unique among integrins (23, 24). Following β4 binding to laminin-5, the distal segment of the large cytoplasmic domain of β4 (referred to herein as the signaling domain) is phosphorylated by a Src family kinase and recruits the signaling adaptor protein Shc, causing activation of Ras and PI-3K (25–28). In addition, the β4 integrin can combine with multiple receptor tyrosine kinases (RTKs) to promote joint signaling (29–32). Intriguingly, in vitro studies have indicated that oncogenic forms of c-Met can induce invasive signaling through phosphorylation of the β4 cytoplasmic domain (30). Furthermore, genetic analysis has revealed that the β4 integrin promotes mammary tumorigenesis by combining with ErbB2 and amplifying its signaling capacity (32). In spite of these advances, it is not clear whether β4 can exert a proneoplastic function in cancers that do not carry activating mutations or genomic amplifications of its partner RTKs, such as prostate carcinomas (5), and, if so, by what mechanism.

In this study, we provide evidence that a significant fraction of human prostate adenocarcinomas and androgen-independent metastases express elevated levels of the β4 integrin. We demonstrate that targeted deletion of the β4 signaling domain inhibits tumor growth and delays tumor progression in PB-*TAg* mice, which undergo prostate-specific inactivation of p53 and Rb, as well as in a allogeneic transplantation model of *Pten* loss-dependent prostate tumorigenesis. We trace this defect back to an inability of signaling-defective β4 to sustain ErbB2 and Met signaling in prostate tumor progenitor cells. Finally, we show that β4 is often coexpressed with c-Met and ErbB2 in human prostate cancers and demonstrate that combined pharmacological inhibition of these RTKs exerts antitumor activity in a xenograft model. These findings indicate that the β4 integrin promotes prostate tumorigenesis by amplifying ErbB2 and c-Met signaling in tumor progenitor cells.

## Results

Human PIN lesions and many invasive prostate cancers express the β4 integrin. To study the expression of the β4 integrin in human prostate cancer, we examined multiple existing DNA microarray data sets using Oncomine 4.4. Since prostate cancer is a biologically and clinically heterogeneous disease, we investigated whether *ITGB4* was overexpressed in a subset of cases by using Cancer Outlier Profile Analysis (COPA), a methodology that has been successful in uncovering candidate oncogenes, such as *ERG* and *ETV1*, in prostate cancer (33). Interestingly, COPA identified *ITGB4* as markedly overexpressed in a subset of tumor samples in 11 out of 16 available data sets (gene rank, top 10%; fold change, >2; $P < 1 \times 10^{-4}$). Using the same statistical filters, *ITGB4* exhibited a COPA score comparable to or higher than that of *ERG* in several data sets (Table 1). Notably, analysis of the LaTulippe data set, which includes 23 primary tumors and 9 metastases (34), indicated that 9.4% of the cases, including the 2 bone metastases present in this data set, were outliers at the 90th percentile (Figure 1A). In agreement with this finding, differential analysis indicated that high-level expression of *ITGB4* was strongly associated with advanced Gleason score in the LaTulippe as well as the Singh data set (34, 35) (Figure 1A and Figure 1B). Taken together, these findings suggest that the β4 integrin is overexpressed in a subset of prostate tumors characterized by an aggressive phenotype.

To examine further the expression of β4 in human prostate cancer, we interrogated a MSKCC DNA microarray data set comprising 23 naive primary prostate cancers, 17 tumors resected after 3 months of androgen ablation therapy, and 9 castration-resistant metastatic lesions (36). LNCaP cells and microdissected normal stroma were used as negative controls, and microdissected normal epithelium was used as a positive control. Whereas a subset of naive primary prostate cancers expressed *ITGB4* at levels comparable to those present in the normal epithelium, a substantial fraction of those resected from patients who had undergone androgen ablation therapy and of those who had developed bone metastases expressed elevated levels of *ITGB4* (Supplemental Figure 1A; supplemental material available online with this article; doi:10.1172/JCI60720DS1). These results suggest that the expression of *ITGB4* is upregulated during progression to castration resistance.

Prior immunohistochemical studies on a small number of frozen low-grade prostate cancer specimens have led to the suggestion that β4 is downregulated during progression to invasive prostate cancer
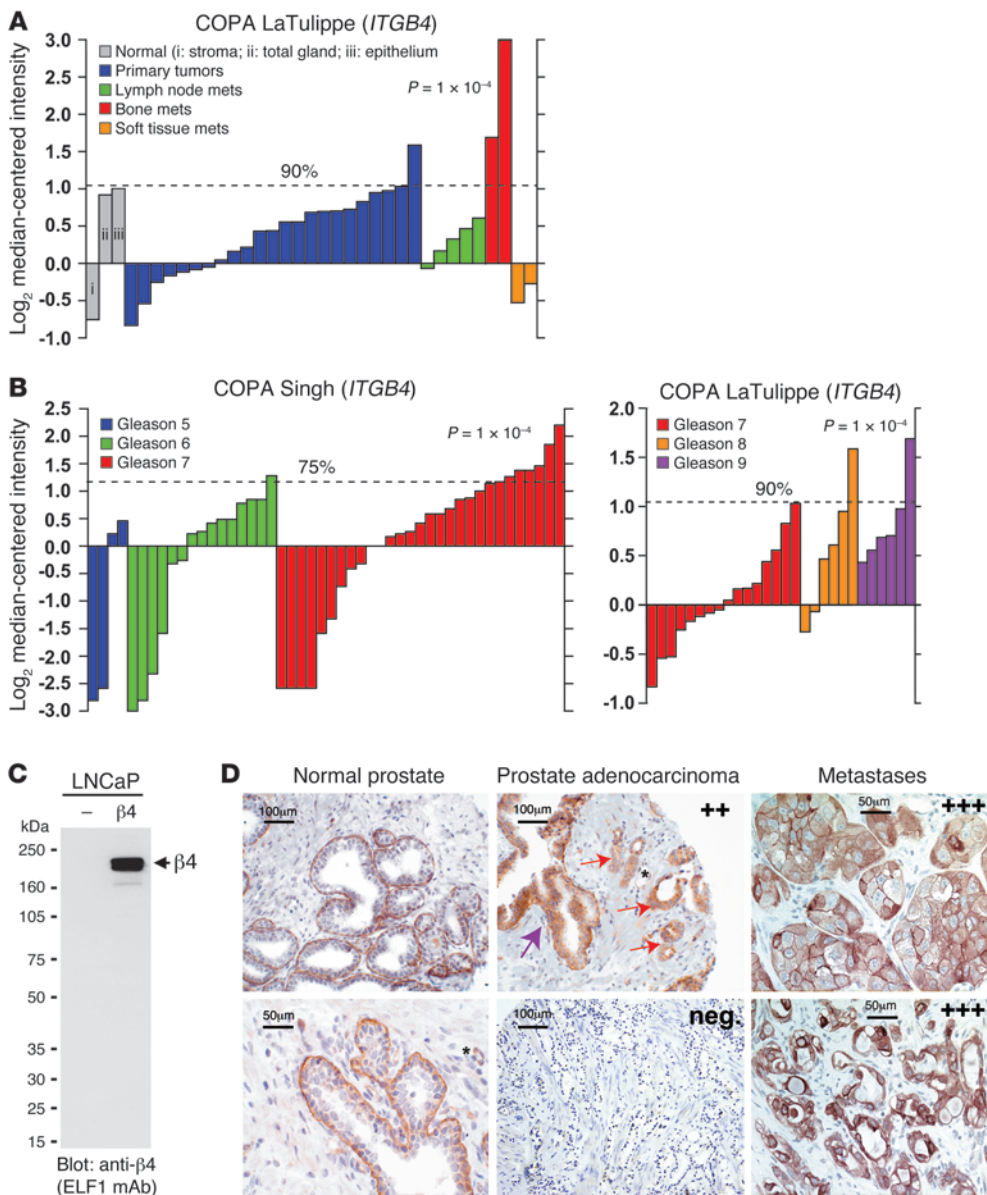
Figure 1
Expression of the β4 integrin in human prostate cancer. (**A**) Summary of COPA of *ITGB4* in 11 prostate cancer DNA microarray data sets (source Oncomine). COPA of *ITGB4* in the LaTulippe data set reveals *ITGB4* as outlier in 2 bone metastases (mets) (34). (**B**) COPA of *ITGB4* in the Singh and LaTulippe data sets (34, 35), in which samples were classified on the basis of Gleason grade. (**C**) Total lysates of LNCaP cells transduced with empty vector or vector encoding human β4 were subjected to immunoblotting with the anti-β4 mAb ELF1. (**D**) Sections from the indicated samples were stained with anti-β4 and counterstained with hematoxylin. The asterisk indicates blood vessels, the purple arrow points to high-grade PIN lesions, and red arrows point to invasive adenocarcinomas. The metastatic lesions are from bone (top) and soft tissue (bottom). The anti-β4 staining intensity of prostate cancer samples was as indicated in the top right corner of each of the relevant panels (neg, negative; ++, moderate; +++, strong). Scale bar: 50 μm (metastases and bottom normal prostate); 100 μm (prostate adenocarcinoma and top normal prostate).

(37). We reasoned that ex vivo proteolysis of β4 by cancer-associated proteases might have interfered with the detection of β4 in these studies. In order to study the expression of β4 under conditions that minimize this potential problem, we developed a protocol of staining with the ELF1 mAb that allows efficient detection of β4 on formalin-fixed and paraffin-embedded sections. Preliminary experiments confirmed that the ELF1 mAb reacts selectively with recombinant human β4 in transfected LNCaP cells (Figure 1C) and that it specifically stains basal cells in normal prostatic glands and endothelial cells in blood vessels (Figure 1D, left, microvessel indicated by asterisk), as anticipated from the known pattern of expression of β4 in the normal human prostate (37). Furthermore, the antibody produced an identical pattern of staining on frozen or paraffin-embedded sections of surgical specimens of prostate cancer that had been selected on the basis of their moderate levels of expression of *ITGB4* mRNA (Supplemental Figure 1, B and C). Pathological diagnosis of prostate cancer had been confirmed by α-methylacyl-CoA racemase staining.

Immunostaining of a tissue microarray (TMA) containing 104 cases of primary prostate cancer indicated that all high-grade PIN lesions expressed elevated levels of β4 (staining intensity, 2+ to 3+) (Supplemental Table 1). In invasive cancer, β4 was expressed not only in residual basal cells but also in neoplastic cells (Figure 1D, top middle panel, purple arrow). Although 65% of invasive carcinomas in this data set exhibited weak or no expression of β4 (staining intensity, 0 to 1+), 35% of these cases expressed elevated levels of β4 (staining intensity, 2+ to 3+) (Supplemental Table 1). Figure 1D includes examples of β4-positive and β4-negative cases (middle panels). Finally, the tumor cells within a large fraction of metastatic lesions (14 out of 36 lymph node, 3 out of 4 soft tissue, 2 out of 4 lung, and 6 out of 31 bone metastases) exhibited high levels of β4 at the cell surface (Figure 1D, right panels).

To validate these results, we tested a second mAb to β4, 439-9B, which has been used to stain paraffin-embedded sections of breast cancer cases (38). This antibody reacted selectively with recombi-

nant human β4 transduced in LNCaP cells (Supplemental Figure 1D) and produced a pattern of staining identical to that generated by the ELF-1 antibody on 2 additional distinct prostate cancer TMAs (Supplemental Figure 1E and Supplemental Tables 2 and 3). Moreover, χ^2 testing indicated that the ELF-1 and 439-9B mAbs generated a similarly intense staining in each case from the 2 data sets. These results reveal that a significant fraction of invasive prostate cancers express elevated levels of the β4 integrin, suggesting that it may play a role in prostate tumor initiation or progression.

Deletion of the β4 signaling domain does not affect prostate development. To examine the role of β4 signaling in prostate tumorigenesis, we decided to cross mice carrying a targeted deletion of the β4 signaling domain (β4$^{1355T/1355T}$ mice; referred to herein as β4-1355T mice) to mice genetically engineered to develop prostate cancer. The β4-1355T mice express a truncated form of the β4 integrin, which retains an intact adhesive function but lacks all major tyrosine phosphorylation sites and is unable to amplify RTK signaling (refs. 32, 39, 40 and Supplemental Figure 2A).

To exclude the possibility that deletion of the β4 signaling domain affects prostate organogenesis, we examined 3-month-old β4-1355T mice. The prostates of these mice weighed as much as those of control mice (data not shown) and appeared macroscopically normal: all lobes were properly developed and had normal relationships with adjacent tissues (Supplemental Figure 2B). Histological analysis did not reveal any differences between β4 mutant and control prostates. Basal and secretory cells had normal morphology, and abundant secretory material was present in the lumen of most glands (Supplemental Figure 2B). Vessels in the stroma were normal in number, distribution, and size (data not shown). The β4 integrin was expressed in basal cells, and laminin-5 was expressed in the basement membrane supporting the secretory cells, as expected. E-cadherin was correctly localized at cell-to-cell junctions. The AR accumulated in the nuclei of secretory cells as well as in stromal cells (Supplemental Figure 2B). In addition, anti-K14 staining indicated that the β4 mutant prostates contain a regular complement of basal cells (data not shown). These results suggest that loss of β4 signaling does not interfere with the specification of different cell types and overall development of the prostate, in agreement with the hypothesis that other laminin-binding integrins may function redundantly during this process.

Loss of β4 signaling inhibits prostate tumorigenesis in PB-TAg mice. To examine the effect of loss of β4 signaling on prostate tumorigenesis, we crossed the mice carrying a targeted deletion of the β4 signaling domain to PB-TAg mice, because this mouse model of prostate tumorigenesis is driven by inactivation of Rb and p53 signaling networks (41, 42), which are commonly inactivated in human prostate cancer (3, 5). Moreover, the PB-TAg mice reproduce several aspects of the histological progression of human prostate cancer, including the expansion of a seemingly luminal compartment expressing the AR (42).

As shown in Figure 2A, deletion of the β4 signaling domain significantly inhibited prostate tumor growth in PB-TAg mice. Prostate expansion became appreciable at 4 months of age in control PB-TAg; β4$^{+/+}$ mice (PB-TAg; β4-WT mice) but only after 6 months in PB-TAg; β4$^{1355T/1355T}$ mice (PB-TAg; β4-1355T mice). At 7 months, the tumors of control mice averaged 6 cm³, whereas those of β4 mutant mice were about 2.5-times smaller. By 8 months, the majority of PB-TAg; β4-WT mice became moribund and had to be sacrificed, precluding a statistically significant measurement of tumor volumes beyond this time point (Figure 2A). In

addition, Kaplan-Meier analysis indicated that the median survival of PB-TAg; β4-1355T mice was prolonged by 2.4 months when compared with that of PB-TAg; β4-WT mice (Figure 2B). These results indicate that deletion of the β4 signaling domain inhibits prostate cancer growth and prolongs survival of PB-TAg mice.

Histological analysis indicated that at 3.5 months of age the majority of PB-TAg; β4-1355T mice exhibited hyperplasia or low-grade PIN and only a small fraction exhibited high-grade PIN. In contrast, a significant fraction of PB-TAg; β4-WT mice had progressed to high-grade PIN and a small percentage of them to well-differentiated carcinoma at this time (Figure 2C). At 5.5 months, the PB-TAg; β4-1355T mice exhibited predominantly high-grade PIN and moderately differentiated and well-differentiated adenocarcinomas. In contrast, a large fraction of PB-TAg; β4-WT mice had poorly differentiated carcinomas (Figure 2C). At 7.5 months, the proportion of various histotypes in both types of mice became similar (Figure 2C), presumably because most of PB-TAg; β4-WT mice carrying advanced tumors had already been sacrificed, whereas the remaining mice carried fewer malignant tumors (Figure 2A). These results suggest that loss of β4 signaling delays histological progression.

Macroscopic and microscopic analysis indicated that the tumors of β4 mutant mice invaded regional lymph nodes much less efficiently as compared with those of control mice. Furthermore, colonization to the lung and liver was substantially delayed in these mice (Figure 2D). Since most metastatic lesions in both PB-TAg; β4-WT and PB-TAg; β4-1355T mice were poorly differentiated (WT mice, 14 out of 14 lymph node, 14 out of 14 lung, and 8 out of 9 liver lesions; 1355T mice, 4 out of 5 lymph node, 6 out of 8 lung, and 6 out of 7 liver lesions), the delay in the outgrowth of metastases in β4 mutant mice likely reflects the slower histological progression of their primary tumors. Interestingly, a similar percentage of PB-TAg; β4-WT and PB-TAg; β4-1355T mice exhibited distant metastases at 8.5 months, consistent with the hypothesis that the small group of PB-TAg; β4-WT mice surviving to this time point carried tumors less malignant than those in the bulk of their cohort but as malignant as those of the majority of PB-TAg; β4-1355T mice, which were still alive at this time point.

Selective expression of the β4 integrin in the basal tumor compartment. To gain insight into the mechanism by which β4 signaling promotes prostate tumorigenesis, we examined the pattern of expression of β4 at various stages of histological progression in PB-TAg mice. We observed that the high-grade PIN lesions arising in these mice retained a substantial number of K14+ basal cells, whereas the invasive edges of the carcinomas did not contain K14+ cells (Figure 3A). In both types of lesion, the K14− neoplastic cells adhering to the basement membrane (heretofore referred to as basal tumor cells) exhibited high levels of β4, whereas those above them (suprabasal tumor cells) expressed much lower levels of the integrin (Figure 3A). In fact, the basal tumor cells exhibited levels of β4 that were much higher than those of normal basal cells (Figure 3B, left row; yellow arrows point to basal cancer cells and white arrows point to normal basal cells). Interestingly, both basal and suprabasal tumor cells expressed high levels of the AR (Figure 3A). Invasive adenocarcinomas retained high-level expression of β4, in spite of a decrease in laminin-5 and E-cadherin staining (Figure 3B). Even cells at the invasive edges of these tumors, which are demarcated by reduced laminin-5 staining, retained expression of β4 (Figure 3B, yellow arrows). In contrast, β4 levels decreased in poorly differentiated, invasive cancers characterized by loss of
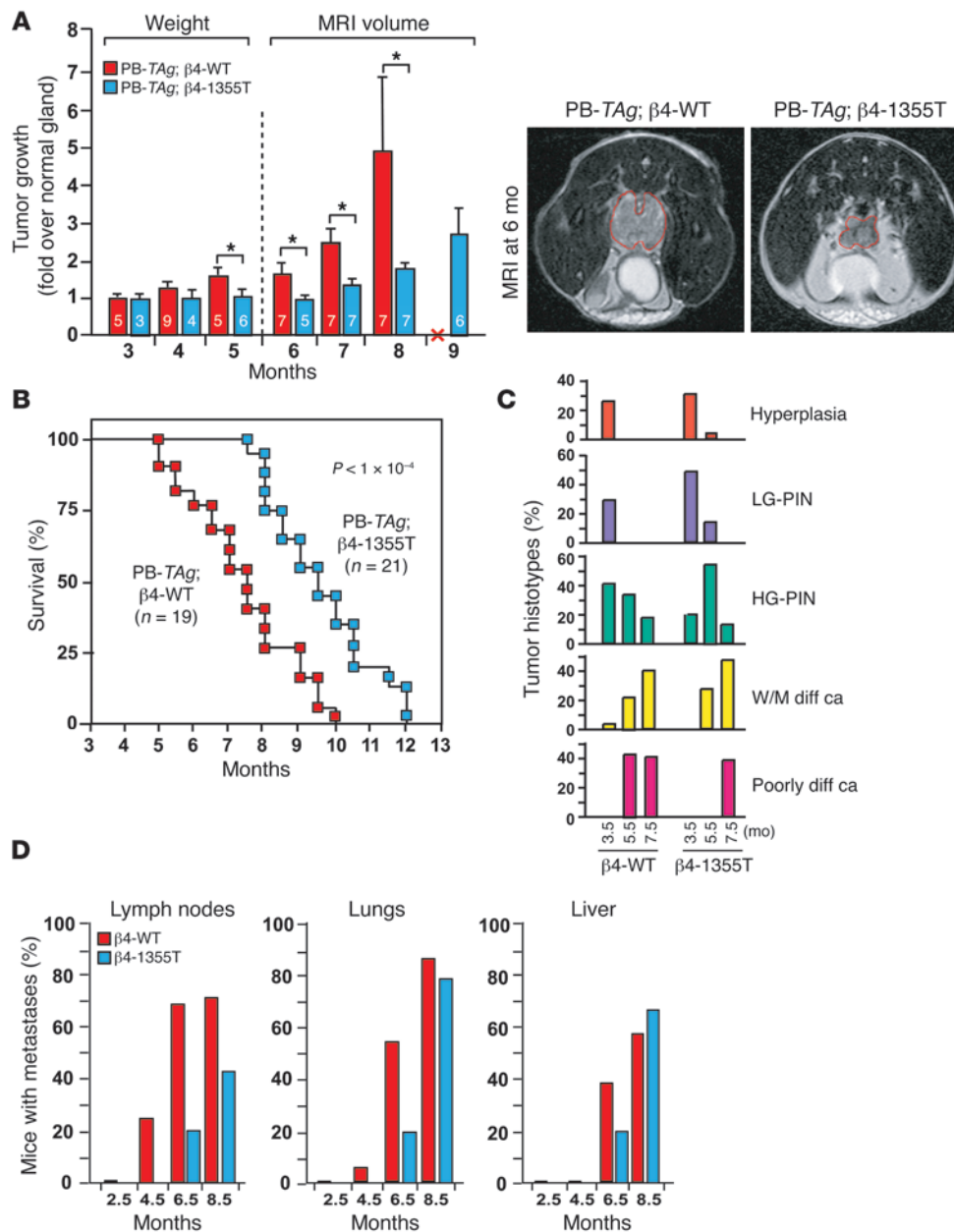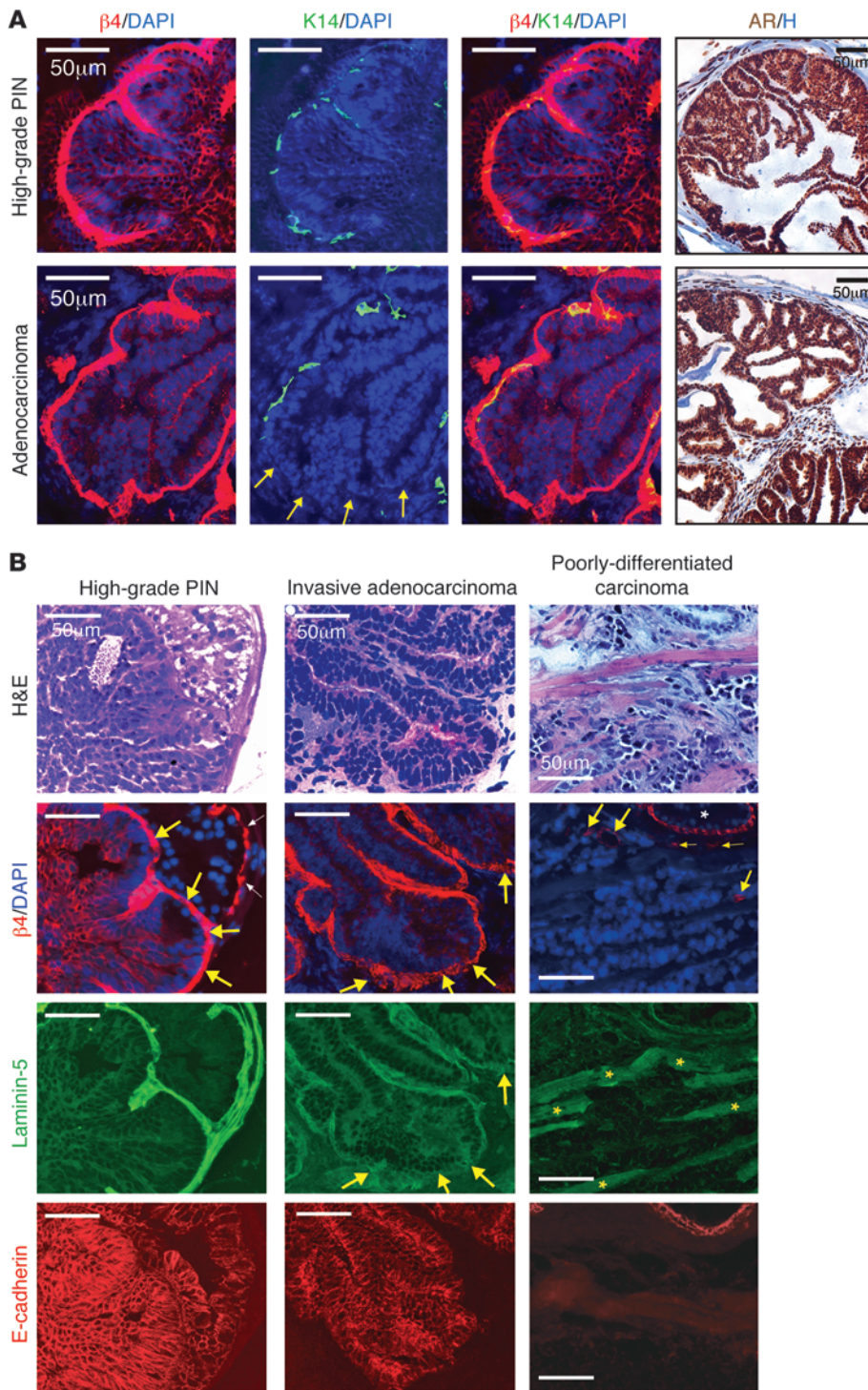
Figure 2

Deletion of the β4 signaling domain inhibits prostate tumorigenesis in PB-*TAg* mice. (**A**) The average primary tumor growth (± SD) in PB-*TAg*; β4-WT and PB-*TAg*; β4-1355T mice. Tumor volumes were determined by excision and weighing up to 5 months of age and by MRI thereafter. Fold increases are over age-matched normal mice. Most PB-*TAg*; β4-WT mice died before 8 months of age, precluding a comparison of tumor growth at 9 months (X). Numbers in columns represent the number of mice. Representative MRI images at 6 months are shown. *$P < 0.002$. (**B**) Kaplan-Meier analysis of survival in the indicated cohorts of mice. (**C**) Distribution of tumor histotypes at the indicated ages. The percentages of hyperplasia, low-grade PIN (LG-PIN), high-grade PIN (HG-PIN), well-differentiated and moderately differentiated carcinoma (W/M diff ca), and poorly differentiated carcinoma (Poorly diff ca) were assessed by double blind histological analysis (PB-*TAg*; β4-WT mice: $n = 10$ at 3.5 months, $n = 14$ at 5.5 months, and $n = 8$ at 7.5 months; PB-*TAg*; β4-1355T mice: $n = 8$ at 3.5 months and $n = 6$ at 5.5 and 7.5 months). $P < 0.0001$ at 5.5 months. (**D**) Percentage of mice that had developed metastatic lesions to lymph nodes, lungs, or liver at the indicated ages (PB-*TAg*; β4-WT: $n = 3$ at 2.5 months, $n = 16$ at 4.5 months, $n = 13$ at 6.5 months, and $n = 7$ at 8.5 months; PB-*TAg*; β4-1355T: $n = 3$ at 2.5 months, $n = 10$ at 4.5 months, $n = 5$ at 6.5 months, and $n = 9$ at 8.5 months).

E-cadherin staining (Figure 3B). Since the poorly differentiated carcinomas, which arise in a fraction of PB-*TAg* mice, exhibit neuroendocrine markers (42), the loss of β4 expression that we observed may be a reflection of this specific tumor progression pathway. In fact, it has been hypothesized that the neuroendocrine tumors of PB-*TAg* mice develop from a distinct progenitor type (43). These results indicate that the basal tumor cells of high-grade PIN lesions and well-differentiated and invasive adenocarcinomas arising in PB-*TAg* mice express elevated levels of the β4 integrin and of the AR. In contrast, the suprabasal tumor cells express much lower levels of β4 but retain expression of the AR. Control experiments indicated that deletion of the signaling domain does not alter the level of expression and subcellular localization of β4 or the TAg in PIN lesions and adenocarcinomas (Supplemental Figure 3, A and B, and data not shown). These results indicate that

deletion of the β4 signaling domain specifically affects prostate tumor initiation and/or progression.

Loss of β4 signaling does not inhibit prostate tumorigenesis by suppressing angiogenesis. Since β4 signaling promotes endothelial cell invasion during neoangiogenesis in certain tumor models (32, 39), we examined whether loss of β4 signaling inhibits tumor angiogenesis in PB-*TAg* mice. The angiogenic switch occurs at the high-grade PIN stage in this mouse model (44), and we found that the high-grade PIN lesions of β4 mutant mice exhibited significantly fewer intraductal microvessels as compared with those of age-matched wild-type β4 mice (Supplemental Figure 4, A and B). However, although the PIN lesions of PB-*TAg*; β4-1355T mice contained a slightly higher number of apoptotic cells as compared with corresponding lesions from PB-*TAg*; β4-WT mice (Supplemental Figure 3C), the percentage of tumor cells undergoing apoptosis

Figure 3
The tumor cells located in the basal compartment of high-grade PIN and invasive adenocarcinomas express elevated levels of the β4 integrin. (**A**) Consecutive sections of high-grade PIN and well-differentiated adenocarcinomas were subjected to double staining with anti-β4 and anti-K14 followed by counterstaining with DAPI. Similar grade histological sections were immunostained for AR and counterstained with H&E. Whereas the PIN lesions retain K14+ basal cells, the adenocarcinomas have lost basal cells (yellow arrows). In both cases, the neoplastic cells adhering to the basement membrane express high levels of β4 as well as the AR. (**B**) Sections of high-grade PIN, invasive adenocarcinoma, and poorly differentiated adenocarcinoma from PB-*TAg*; β4-WT mice were stained with H&E, DAPI, and antibodies to β4, laminin-5, or E-cadherin. In PIN lesions, prostate carcinoma cells adhering to laminin-5 express high levels of β4 (yellow arrows), whereas suprabasal cells express lower levels of the integrin. The white arrows indicate the β4-positive basal cells beneath the basement membrane of adjacent normal gland. The β4 integrin continues to be expressed at high levels in invasive adenocarcinomas. At invasion fronts (yellow arrows), β4 losses its basal concentration and the staining for laminin-5 becomes fragmented. The poorly differentiated adenocarcinomas arising in this model exhibit neuroendocrine features. In these lesions, β4, E-cadherin, and laminin-5 are no longer detectable. β4 is still expressed in blood vessels (yellow arrows). The white asterisk marks a normal gland, and yellow asterisks mark laminin-5–positive muscle fibers. Scale bar: 50 μm.

in these lesions was very low in both genotypes (<2%). In addition, we did not detect elevated levels of hypoxia-induced Glut1 or histological signs of necrosis in the PIN lesions of β4 mutant mice (Supplemental Figure 4D and data not shown). Finally, we did not detect differences in neoangiogenesis when we grouped the samples according to histological classification instead of age (Supplemental Figure 4E), suggesting that the difference in neoangiogenesis observed in age-matched mice was largely attributable

to a slower histological progression of the high-grade PIN lesions of β4 mutant mice. These results suggest that loss of β4 signaling does not impair prostate tumor growth and histological progression by reducing tumor angiogenesis but rather by a tumor cell-intrinsic mechanism.

Integrin β4 signaling promotes self-renewal of tumor progenitor cells and rapid proliferation of transit-amplifying tumor cells. To examine the effect of β4 signaling on tumor cell proliferation, we subjected

high-grade PIN lesions and well-differentiated adenocarcinomas from PB-*TAg* mice expressing wild-type or mutant β4 to anti–Ki-67 staining. Examination of control lesions indicated that the tumor cells adhering to the basement membrane proliferate at a much higher rate compared with those above them, in agreement with the hypothesis that integrin-mediated adhesion promotes mitogenic signaling (Figure 4A, top). Notably, the proliferative index of advanced PIN lesions and well-differentiated adenocarcinomas from mice expressing mutant β4 was significantly lower than that of histologically similar lesions from control mice, suggesting that β4 signaling promotes tumor cell proliferation (Figure 4, A and B).

To directly examine this hypothesis, we used in vivo DNA labeling with 5-ethynyl-2′-deoxyuridine (EdU). PB-*TAg*; β4-WT and PB-*TAg*; β4-1355T mice were injected with EdU daily for 3 days prior to isolation of prostate cells. FACS analysis indicated that most of the tumor cells that incorporated EdU over the 3-day period in both types of mice were β4$^+$, in agreement with the conclusion that tumor cell proliferation is restricted to the subpopulation of tumor cells expressing the β4 integrin and adhering to the basement membrane (Figure 4C). Interestingly, the β4$^+$ tumor cells from PB-*TAg*; β4-1355T mice incorporated EdU in vivo at a severely reduced rate as compared with that of relative controls, indicating that deletion of the β4 signaling domain suppresses the proliferative potential of this compartment (Figure 4C). In spite of this significant proliferative impairment, tumors arising in β4 mutant mice did not exhibit a lower proportion of β4$^+$ cells as compared with tumors of similar histology arising in control mice (data not shown), suggesting that defective proliferation is accompanied by defective transit into more a differentiated compartment in β4 mutant mice. These results provide evidence that β4 signaling promotes prostate tumor growth by enhancing the proliferation of tumor cells that have characteristics similar to those of transit-amplifying cells.

Prospective identification experiments have indicated that the basal compartment of the mouse prostate contains a subpopulation of stem cells that express Sca-1 and high levels of CD49 (α6 integrin) and can initiate prostate tumorigenesis (17, 45). We have recently observed that these normal stem cells express the β4 integrin, but not α6β1, and they can therefore be better identified using Sca-1 and β4 as markers (J. Otero et al., unpublished observations). To examine the expression and signaling function of the β4 integrin in prostate tumor progenitor cells, we used flow cytometry to sort tumor cells from PB-*TAg*; β4-WT and PB-*TAg*; β4-1355TT mice into 4 subpopulations characterized by differential expression of Sca-1 and β4 and subjected them to prostatosphere assays. Dissociated tumor cells were depleted of endothelial cells and leukocytes (Lin$^-$) and sorted into Sca-1^{hi} (single Sca-1$^+$ cells), β4^{hi}Sca-1^{hi} (double-positive [DP] cells), β4^{hi}Sca-1^{lo} (single β4$^+$ cells), and β4^{lo}Sca-1^{lo} (double-negative [DN] cells) subpopulations (Figure 4D). Since the DN cells comprise also stromal cells, the epithelial cells in this subpopulation were further sorted using anti-EpCAM. Upon plating on nonadherent plates, the DP cells from PB-*TAg*; β4-WT mice exhibited a significantly higher capacity to form prostatospheres as compared with the other subpopulations of tumor cells, suggesting that the DP tumor cells possess self-renewal capability (Figure 4E, left). Notably, the DP tumor cells from β4 mutant mice formed significantly fewer prostatospheres as compared with the control DP wild-type cells (Figure 4E, right), suggesting that deletion of the β4 signaling domain inhibits the ability of tumor progenitor cells to undergo self-renewal in vitro.

To test whether loss of β4 signaling affects the ability of tumor progenitor cells to seed tumors in vivo, we implanted 50,000 freshly sorted Sca-1$^+$ single-positive, DP, β4$^+$ single-positive, or DN EpCAM$^+$ cells from PB-*TAg*; β4-WT or PB-*TAg*; β4-1355T tumors into the anterior prostate of NOD/SCID/*Il2rg*$^{-/-}$ mice. Ninety days later, the mice were sacrificed and prostate sections were subjected to immunohistochemistry for large TAg to identify secondary lesions. The results indicated that the DP and single β4$^+$ cells from PB-*TAg*; β4-WT mice were able to form, albeit at a very low frequency, secondary tumors that contained areas of high-grade PIN and adenocarcinomas (Supplemental Figure 5A, top row), suggesting that the β4$^+$ tumor cells comprise progenitors endowed with transplantation capacity. In contrast, none of the cells from PB-*TAg*; β4-1355T mice were able to initiate secondary tumors under the same conditions (Supplemental Figure 5A, bottom row). These observations suggest that loss of β4 signaling inhibits the ability of putative cancer stem cells and transit-amplifying cells to initiate secondary tumors in vivo.

To examine the hypothesis that β4 signaling promotes tumor initiation, we examined the effect of prostate epithelial-specific deletion of the β4 signaling domain on oncogenesis driven by inactivation of *Pten*, a common lesion in human prostate cancer. Prostate epithelial cells derived from β4 wild-type and mutant mice were infected with lentiviruses encoding an shRNA targeting Pten, mixed with embryonic rat urogenital sinus mesenchymal cells, and injected under the renal capsule under conditions that are state of the art for the evaluation of cancer stem cell potential (16, 45, 46). Whereas the β4 wild-type tumor cells formed numerous, large PIN lesions as well as normal glands, the β4 mutant cells generated only a few, small PIN lesions against a similar background of normal glands (Figure 4, F and G). Interestingly, the PIN lesions generated by β4 mutant cells displayed reduced P-AKT staining as compared with similarly sized control lesions (Supplemental Figure 5B). These observations suggest that β4 signaling promotes prostate tumor initiation in a model driven by inactivation of Pten. Taken together, these findings suggest that the β4 integrin promotes prostate tumor growth by enhancing the self-renewal capability of putative stem cells and rapid proliferation of transit-amplifying cells.
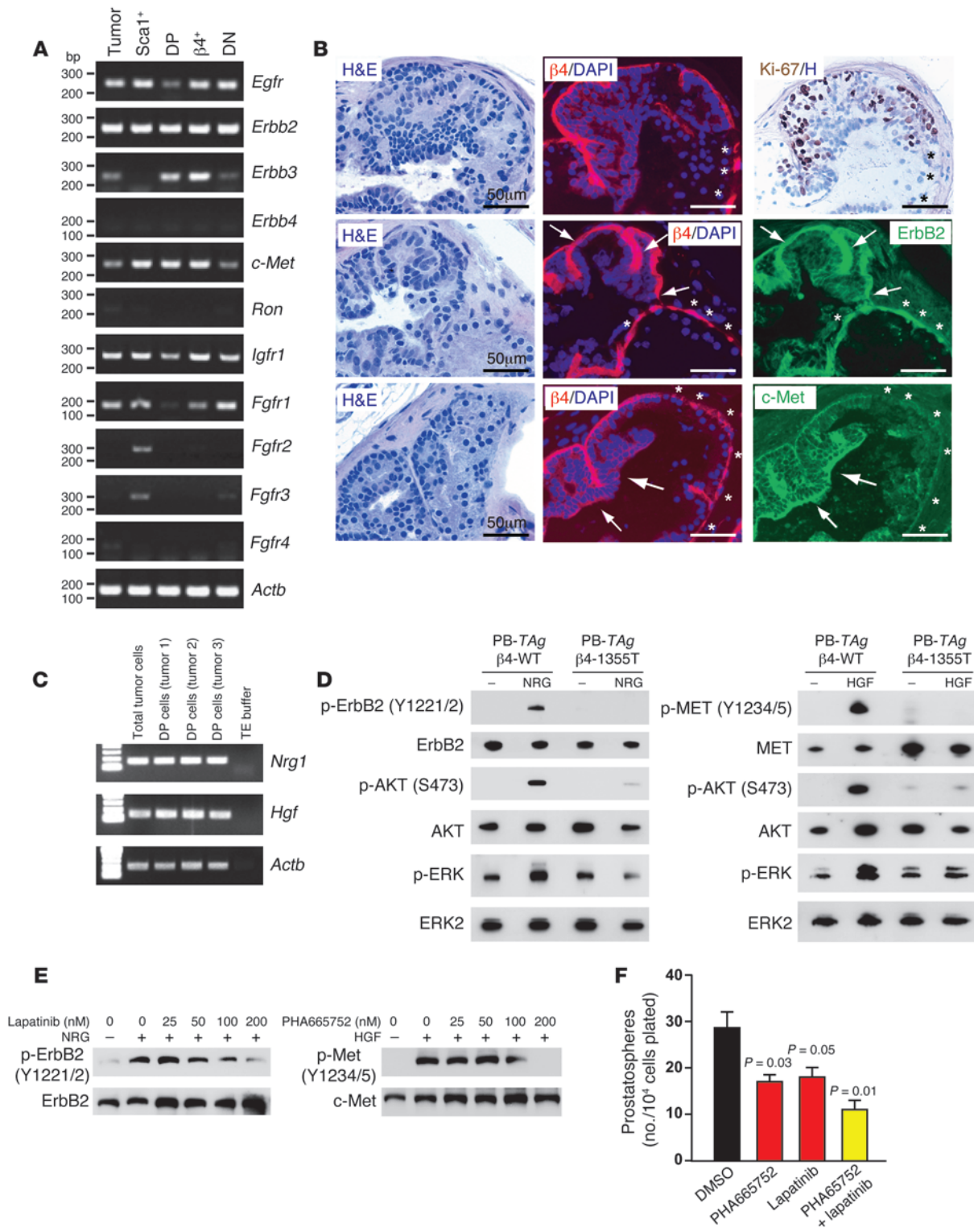
The β4 integrin amplifies ErbB2 and Met signaling in prostate tumor progenitor cells. The β4 integrin potentiates signaling by multiple RTKs, including ErbB2 and c-Met (47), which have been implicated in human prostate tumorigenesis (48, 49). To obtain insight into the mechanism by which β4 promotes the expansion of tumor progenitor cells, we examined the level of expression of a panel of RTKs in Sca-1$^+$ (β4$^-$), DP, β4$^+$ (Sca-1$^-$), and DN cells isolated from PB-*TAg* tumors. Semiquantitative RT-PCR indicated that the DP tumor cells express ErbB2 and ErbB3 and low levels of EGFR but not ErbB4. In addition, these cells expressed c-Met, but not RON, and low levels of IGF-R1 and FGF-R1 but not FGF-R2, FGF-R3, or FGF-R4 (Figure 5A). Immunofluorescent staining confirmed the expression of ErbB2 and c-Met in the high-grade PIN lesions of PB-*TAg* mice (Figure 5B). Whereas ErbB2 was concentrated at the basal surface of tumor cells adhering to the basement membrane, Met was also expressed in suprabasal tumor cells (Figure 5B). High-grade PIN lesions from β4 mutant mice exhibited a similar pattern of staining (data not shown). Interestingly, the DP cells expressed neuregulin-1 (NRG-1; which binds to ErbB2/ErbB3 dimers) and HGF (c-Met ligand), suggesting that autocrine stimulation can sustain ErbB2 and c-Met signaling in these cells (Figure 5C). These
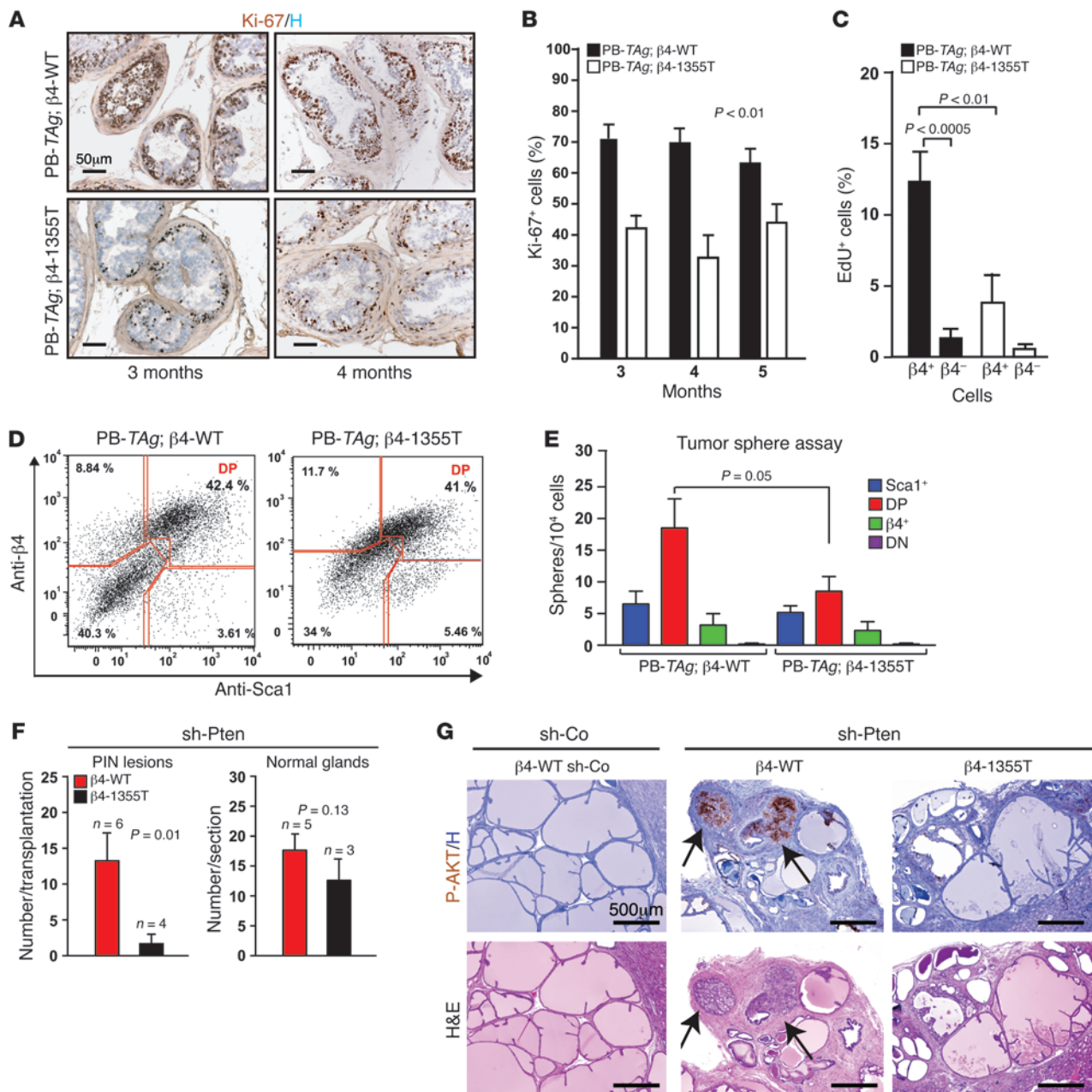
Figure 4
Deletion of the β4 signaling domain inhibits the manifestation of cancer stem cell traits. (**A**) High-grade PIN lesions from 3- and 4-month-old PB-*TAg*; β4-WT and PB-*TAg*; β4-1355T mice were stained with anti–Ki-67 and counterstained with hematoxylin (H). Scale bar: 50 μm. (**B**) The mean percentage of Ki-67–positive cells (± SD) at the indicated times (*n* = 3 per group). (**C**) Mice were injected with EdU for 3 consecutive days. Lin⁻ cells were stained for β4 and EdU and analyzed by FACS. The graph shows the mean (± SEM) percentage of EdU⁺ cells in the indicated subpopulations of cells (*n* = 4 per group). (**D**) Tumors cells from 4.5-month-old PB-*TAg*; β4-WT and 6.5-month-old PB-*TAg*; β4-1355T mice were sorted into 4 subpopulations after gating for Lin⁻ cells. EpCAM⁻ cells were excluded from the DN cells. (**E**) The mean (± SEM) spheres (*n* = 6 per group). (**F**) Prostate epithelial cells from β4-WT and β4-1355T mice were infected in vitro with a lentiviral vector encoding a shRNA targeting *Pten* and xenotransplanted together with urogenital sinus mesenchymal cells under the renal capsule of NOD/SCID/*Il2rg*⁻/⁻ mice. The graphs show the mean (± SD) number of PIN lesions per transplanted kidney and the mean (± SD) number of normal glands per section (right). (**G**) Sections across the subcapsular injection site were stained with anti–P-AKT and counterstained with hematoxylin. Adjacent sections were stained with H&E. Arrows point to PIN lesions exhibiting high-level activation of AKT. Representative images are shown. Scale bar: 500 μm.

Figure 5

The β4 integrin amplifies ErbB2 and c-Met signaling in tumor progenitor cells. (**A**) Dissociated total tumor cells and the indicated subpopulations from 4.5-month-old PB-*TAg*; β4-WT mice were subjected to semi-quantitative RT-PCR to assess expression of the indicated mRNAs. (**B**) Adjacent sections of high-grade PIN lesions from PB-*TAg*; β4-WT mice were stained with H&E and antibodies to β4, followed by counterstaining with DAPI, and anti-Ki-67, followed by counterstaining with hematoxylin, anti-ErbB2, or anti-c-Met. Basal tumor cells in high-grade PIN lesions (arrows) express elevated levels of β4 and ErbB2 as compared with normal basal cells (asterisk). The levels of c-Met are increased in both basal and suprabasal tumor cells (arrows). Scale bar: 50 μm. (**C**) DP cells from 3 tumors arising in 4.5-month-old PB-*TAg*; β4-WT mice were subjected to semiquantitative RT-PCR to assess expression of the indicated mRNAs. Total tumor cells served as positive controls. (**D**) β4-positive cells were sorted from 4.5-month-old PB-*TAg*; β4-WT and 6.5-month-old PB-*TAg*; β4-1355T mice after gating for Lin⁻ cells, plated on laminin-5–coated plates, and stimulated or not with HGF or NRG-1 for 20 minutes. Equal amounts of total protein were subjected to immunoblotting. (**E**) DU145 cells were treated with varying concentrations of lapatinib (EGFR/HER2 inhibitor) or PHA665752 (c-Met inhibitor) and subjected to immunoblotting. (**F**) DP cells from PB-*TAg*; β4-WT mice were assayed for sphere-forming capability in the presence of 100 nM PHA665752, 100 nM lapatinib, or both. The graph shows the mean (± SEM) number of spheres per 10,000 cells after 12 days of culture.

results raise the hypothesis that β4 cooperates with ErbB2 and c-Met to promote the expansion of putative stem cells and transit-amplifying cells located in the basal layer of prostate tumors.

To examine whether the β4 integrin amplifies ErbB2 or c-Met signaling in primary prostate tumor cells, β4⁺ tumor cells isolated from PB-*TAg*; β4-WT and PB-*TAg*; β4-1355T mice were plated on laminin-5 and treated with either NRG or HGF. Immunoblotting revealed that the tumor cells isolated from β4 mutant mice exhibited reduced activation of ErbB2 and c-Met and defective downstream signaling to AKT and ERK in response to stimulation by their cognate ligands (Figure 5D). These results suggest that the β4 signaling domain potentiates ErbB2 and Met signaling in prostate tumor cells.

To assess the biological significance of ErbB2 and c-Met signaling in prostate tumor progenitor cells, we treated DP tumor cells from PB-*TAg*; β4-WT mice with the c-Met inhibitor PHA665752, the ErbB2/EGFR inhibitor lapatinib, or a combination of both inhibitors. The inhibitors were used at 100 nM, a concentration just above their apparent IC₅₀ in DU145 prostate carcinoma cells (Figure 5E). Interestingly, whereas each of the 2 compounds inhibited the ability of DP cells expressing wild-type β4 to form prostatospheres in vitro to a similar extent, the combination of the 2 inhibitors displayed a higher efficacy (Figure 5F). Notably, pharmacological inhibition of ErbB2 and c-Met inhibited the self-renewal capacity of DP tumor cells as efficiently as deletion of the β4 signaling domain did in the same cells (compare Figure 4E and Figure 5F). These findings indicate that inhibition of joint β4-ErbB2/c-Met signaling reduces the self-renewal capacity of prostate tumor progenitor cells.

To evaluate the generality of these findings, we examined 2 additional mouse models of prostate cancer: the ARR2PB-*Myc* (Hi-*Myc*) mice, which overexpress c-Myc in their prostate epithelium (50), and the PB-*Cre4*; *Pten^fl/fl^* (*Pten^PC/PC^*) mice, which carry a prostate-specific inactivation of PTEN (51). Semiquantitative RT-PCR indicated that the DP tumor cells isolated from Hi-*Myc* and *Pten^PC/PC^*

mice express high levels of ErbB2/ErbB3 and c-Met (Supplemental Figure 6A). In addition, upon plating on nonadherent plates, the DP cells from both types of mice formed prostatospheres (Supplemental Figure 6B) as efficiently as those isolated from PB-*TAg* mice (Figure 4E). Finally, PHA665752 and lapatinib inhibited the ability of DP cells from Hi-*Myc* and *Pten^PC/PC^* mice to undergo self-renewal in vitro, although they did not produce an additive or synergistic effect when used in combination (Supplemental Figure 5B). These results suggest that joint β4-ErbB2/c-Met signaling promotes the expansion of tumor progenitor cells independently of the specific underlying oncogenic mutation.

The β4 integrin amplifies ErbB2 and c-Met oncogenic signaling in human prostate carcinoma cells. To study the role of β4 in human prostate tumorigenesis, we examined the expression of β4, ErbB2, ErbB3, EGFR, and c-Met in a panel of human prostate carcinoma cell lines. We found that the androgen-dependent, luminal-like LNCaP and VCaP cells do not express readily detectable levels of β4. In contrast, the androgen-independent DU145, PC3, and PC3M cells expressed high levels of β4 (Figure 6A). In agreement with prior results (49, 52), both androgen-independent and luminal-like cells expressed ErbB2 and — with the exception of LNCaP cells — EGFR, whereas the androgen-independent cell lines exhibited high levels of c-Met. Furthermore, the expression of ErbB3 was restricted to LNCaP and DU145 cells (Figure 6A). Interestingly, the normal prostate epithelial cells, PrEC cells, which possess a phenotype similar to basal-like transit-amplifying cells (53, 54), were found to express high levels of β4 and a repertoire of RTKs similar to those of androgen-independent prostate carcinoma cell lines (Figure 6A).

To examine the mechanism by which the β4 integrin promotes ErbB2 and c-Met signaling, we silenced β4 expression in DU145 cells, because these cells express ErbB2/ErbB3 and c-Met, similar to the DP tumor progenitor cells isolated from PB-*TAg*, Hi-*Myc*, and *Pten^PC/PC^* mice. In addition, the DU145 cells expressed high levels of CD44 and Trop2 (Figure 6B), like the recently characterized human prostate stem cells (16), and have additional attributes of cancer stem cells (55). Immunoprecipitation experiments indicated that β4 combines with ErbB2 and c-Met in DU145 cells. As anticipated, knockdown of β4 led to depletion of total β4 (Figure 6C, top) as well as a disappearance of ErbB2 and c-Met from β4 immunoprecipitates, supporting the specificity of the coimmunoprecipitation observed in control cells expressing β4 (Figure 6C, bottom). Notably, silencing of β4 suppressed NRG-induced phosphorylation of ErbB2 at Tyr 877, which is located in the P loop and is involved in kinase activation, and at Tyr 1248, which mediates recruitment of Shc (ref. 56 and Figure 6D). In addition, knockdown of β4 inhibited HGF-induced phosphorylation of c-Met at Tyr 1349, which is involved in activation of Ras- and PI3K-dependent pathways (ref. 57 and Figure 6D). These results suggest that the β4 integrin promotes ErbB2 and c-Met signaling in human prostate cancer cells.

To examine the functional consequences of depletion of β4, we first compared the ability of control and β4-silenced DU145 cells to proliferate and invade in vitro. BrdU incorporation experiments showed that knockdown of β4 suppresses the ability of DU145 cells to undergo mitogenesis in response to NRG and HGF, but it does not affect FBS-induced cell proliferation to a significant extent (Figure 6E). In addition, Matrigel invasion assays indicated that silencing of β4 inhibits invasion in vitro in response to NRG and HGF but not FBS (Figure 6F). These results suggest that β4 cooperates with ErbB2/3 and Met to promote prostate carcinoma cell proliferation and invasion in vitro.
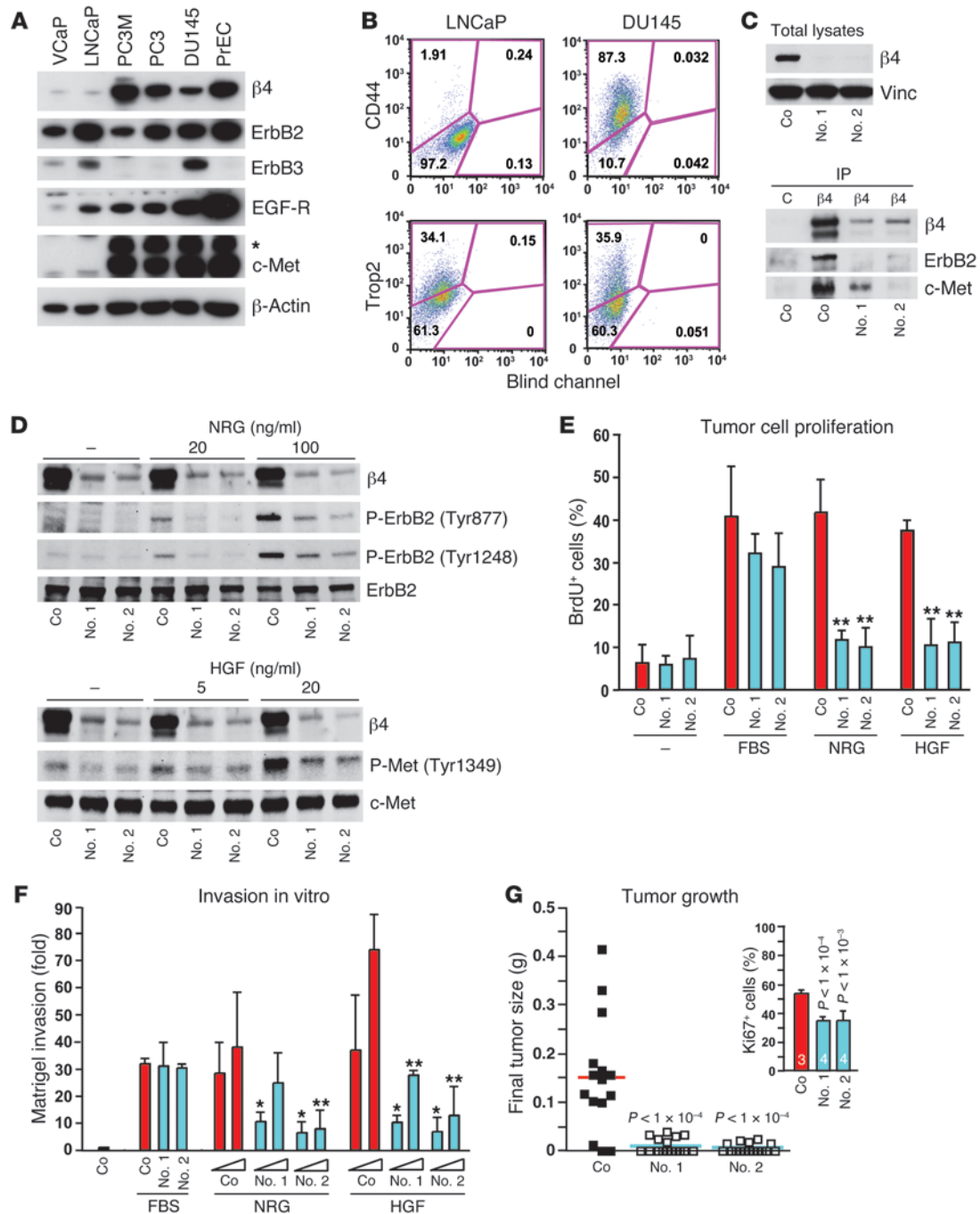
Figure 6

Silencing of β4 suppresses ErbB2 and c-Met signaling and inhibits the oncogenic behavior of castration-resistant human prostate cancer cells. (A) Total proteins from the indicated cells lines were subjected to immunoblotting. The asterisk indicates the c-Met precursor. (B) FACS analysis of CD44 and Trop2 in LNCaP and DU145 cells. (C) DU145 cells were transduced with a control shRNA (Co) or 2 shRNAs targeting β4 (no. 1 and no. 2). Lysates were subjected to immunoblotting (top) or immunoprecipitated with control or anti-β4 antibodies followed by immunoblotting (bottom). Vinc, Vinculin. (D) Control and β4-silenced DU145 cells were treated with NRG or HGF for 30 minutes and subjected to immunoblotting. (E) The indicated cells were synchronized by a double block with 1 mM hydroxyurea; deprived of growth factors; treated with serum-free medium (−), 10% FBS, 10 ng/ml HGF, or 10 ng/ml NRG for 10 hours; and subjected to BrdU incorporation assay. The graph represents (mean ± SD) the percentage of BrdU+ cells. **$P < 0.01$. (F) The indicated cells were subjected to Matrigel invasion assay. 10% FBS, 10 or 100 ng/ml NRG, and 10 or 100 ng/ml HGF were used as chemoattractants. The graph shows the mean fold invasion (± SD) over control. *$P < 0.05$; **$P < 0.01$. (G) The indicated cells were injected subcutaneously in nude mice. The graph shows the average tumor weight (indicated by horizontal lines) 32 days after injection. Symbols on the baseline indicate injections that did not generate tumors. The inset shows the mean percentage of Ki-67+ tumor cells (± SD) in the indicated xenografts. Numbers in columns represent the number of mice.

To examine the effect of β4 on tumorigenicity, control and β4-silenced DU145 cells were injected subcutaneously in nude mice. The β4-silenced cells formed subcutaneous tumors much less efficiently as compared with control cells expressing endogenous β4. In addition, these tumors grew to a significantly smaller size as compared with controls (Figure 6G). Anti–Ki-67 staining of tumor sections indicated that this effect was at least in part attributable to decreased tumor cell proliferation (Figure 6G, insert). Thus, knockdown of β4 suppresses DU145 tumor cell growth in vivo. Together, these results suggest that the β4 integrin enhances human prostate cancer cell proliferation, invasion, and tumorigenicity by amplifying RTK signaling.

To further examine the effect of β4 on human prostate carcinoma cells, we expressed β4-WT or β4-1355T in LNCaP cells at levels similar to those of endogenous β4 in HaCat keratinocytes (Supplemental Figure 7A). In agreement with prior results indicating that ErbB2/ErbB3 induces phosphorylation of the β4 signaling domain (32), immunoprecipitation and immunoblotting showed that NRG promotes tyrosine phosphorylation of wild-type but not of mutant β4 (Supplemental Figure 7B). NRG induced a higher level of phosphorylation of ErbB2 and recruitment and phosphorylation of the 66-kDa isoform of Shc in LNCaP cells expressing wild-type β4 than it did in those expressing β4-1355T or no β4 (Supplemental Figure 7C). Since p66 Shc mediates proliferative signaling in LNCaP cells (58), these observations suggest that the β4 signaling domain promotes activation of ErbB2 and downstream mitogenic signaling through p66 Shc. In addition, NRG activated ERK and JNK more potently in cells expressing wild-type β4 than it did in those expressing β4-1355T or no β4 (Supplemental Figure 7D). β4 signaling did not affect activation of Akt, presumably because LNCaP cells lack PTEN and thus display constitutive activation of PI-3K (59). These experiments indicate that β4 can also potentiate ErbB2 signaling in androgen-dependent cells.

Cell proliferation assays indicated that LNCaP cells expressing wild-type β4 proliferate in vitro at a rate higher than control cells or those expressing β4-1355T, both in the absence and in the presence of NRG1 (Supplemental Figure 7E). The ability of β4 signaling to promote LNCaP mitogenesis also in the absence of exogenous growth factors is consistent with the existence of an autocrine loop involving ErbB receptors in these cells (60). Finally, upon subcutaneous injection in nude mice, LNCaP cells expressing wild-type β4 formed tumors about 2-fold larger than those generated by LNCaP cells expressing similar levels of β4-1355T or no β4 (Supplemental Figure 7F). Anti–Ki-67 staining of tumor sections indicated that this effect was attributable to increased tumor cell proliferation (Supplemental Figure 7G). These results indicate that expression of β4 enhances the ability of LNCaP cells to form tumors upon xenotransplantation in nude mice. Taken together, the results of silencing and positive expression support the hypothesis that the β4 integrin sustains the oncogenic behavior of human prostate cancer cells by amplifying ErbB2 and c-Met signaling.
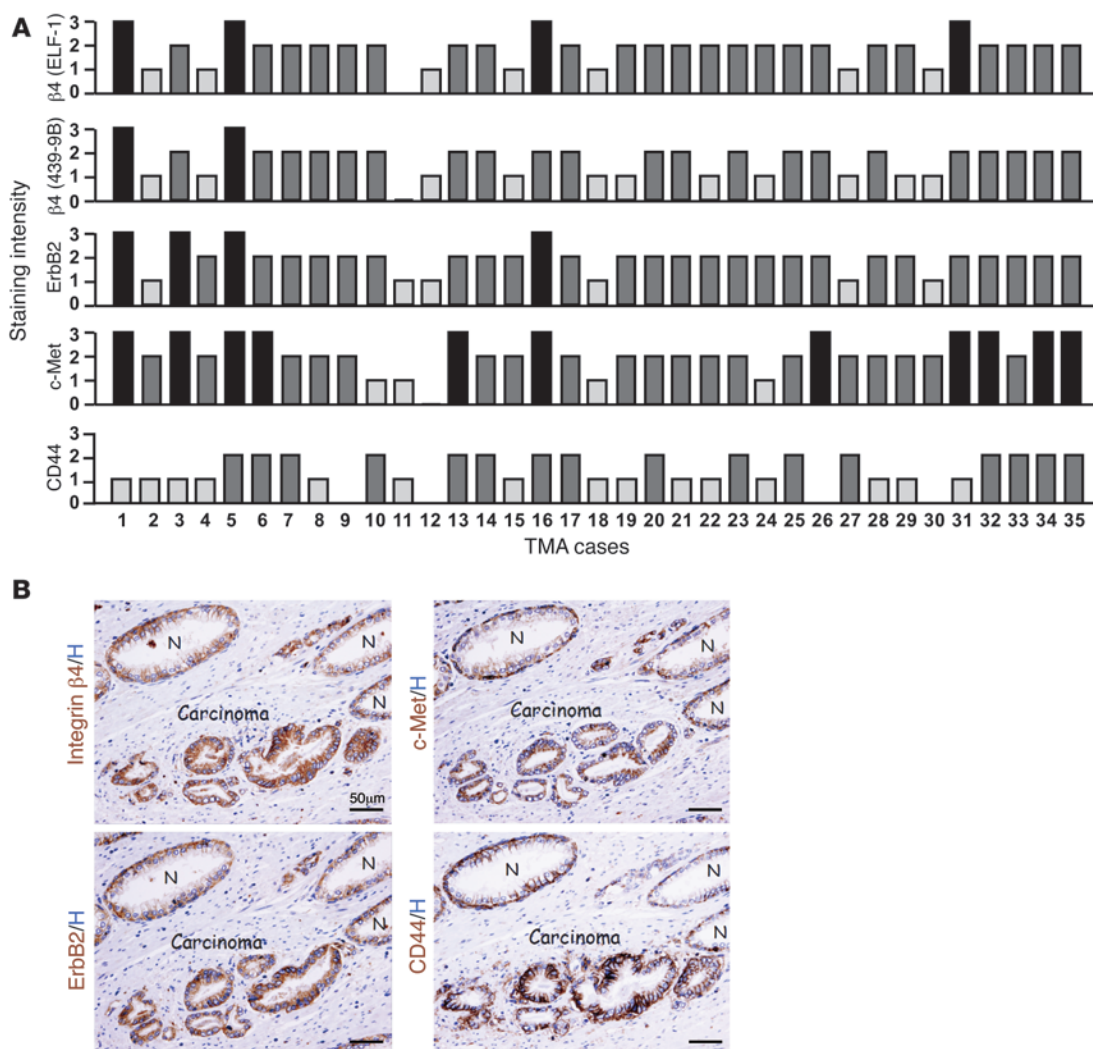
The β4 integrin is coexpressed with ErbB2 and c-Met in human prostate cancer cells. We reasoned that the elevated expression of β4 in a subset of invasive prostate cancers (Figure 1, Supplemental Figure 1, and Supplemental Tables 1–3) might reflect a higher proportion of basal-like tumor progenitor cells in these tumors. Interestingly, coexpression analysis of the Wallace data set (61) revealed that the expression of ITGB4 correlated positively with that of several genes known to be expressed in basally localized transit-amplifying cells and in cells of intermediate phenotype, such as TP63, KRT5 (encod-

ing keratin 5), LAMB3 (encoding the laminin-5 β3 subunit) (correlation coefficient [CC], 0.83), and MET (CC, 0.39) ($P < 1 \times 10^{-6}$). Examination of the Glinsky data set validated these correlations (TP63 CC, 0.8; KRT5 CC, 0.79; LAMB3 CC, 0.77; MET CC, 0.56) ($P < 1 \times 10^{-6}$) (62). Moreover, the expression of ITGB4 strongly correlated with that of KRT15 (encoding keratin 15) in multiple data sets (as published by Vanaja [CC, 0.87, ref. 63]; Wallace [CC, 0.83, ref. 61]; Glinsky [CC, 0.79, ref. 62]; the Bittner data set [CC, 0.4, GEO accession no. GSE2109]). Intriguingly, keratin 15 marks hair follicle stem cells, which function as the cells of origin in basal cell carcinomas arising in $Ptch1^{+/-}$ mice, and is enriched in human mammary progenitor cells (64, 65). Taken together, these findings suggest that the β4 integrin is expressed in prostate tumors containing a high percentage of basal-like progenitor cells and are consistent with the hypothesis that β4 promotes a more aggressive phenotype.

To examine whether β4 was coexpressed with ErbB2 and Met in individual tumor cells, we examined a TMA data set, including 35 primary adenocarcinomas, representing varying pathological grades and clinical stages (Supplemental Tables 4 and 5). Interestingly, virtually all of the cases that were moderately or strongly positive for β4 staining were also moderately or strongly positive for ErbB2 (23 out of 35), c-Met (22 out of 35), or both RTKs (22 out of 35) (Figure 7A). Since CD44 can be used in conjunction with other markers to identify human prostate cancer progenitor cells (66, 67), we also examined its expression in the microarray data set. High-level expression of CD44 correlated with high-level expression of β4, ErbB2, and c-Met in a large fraction of samples (14 out of 22) (Figure 7A). Examination of the samples indicated that β4, ErbB2, and c-Met were expressed at similar levels in most tumor cells, whereas the levels of expression of CD44 were more variable (Figure 7B, labeled Carcinoma; Supplemental Figure 8). As anticipated, the 4 proteins were coexpressed in normal basal cells but not in luminal cells in unaffected glands (Figure 7B, labeled N), suggesting that they define a human basal compartment that includes both stem cells and transit-amplifying cells. χ^2 testing indicated that the correlation of the expression of β4 with that of ErbB2 ot c-Met was statistically significant, whereas that of β4 with CD44 was not. Taken together, these results suggest that the β4 integrin is coexpressed with ErbB2 and c-Met in a subpopulation of tumor cells that may include putative stem cells and transit-amplifying cells and may be expanded in aggressive forms of prostate cancer.

Combined pharmacological inhibition of HER2 and c-Met exhibits antitumor activity in vivo. To begin to assess the potential therapeutic relevance of our findings, we evaluated whether combined inhibition of ErbB2 with lapatinib (68) and c-Met with crizotinib (69) exerted antitumor activity in the DU145 xenograft model. We chose these drugs because they are approved for clinical use. To improve tumor initiation, the tumor cells were injected in NOD/SCID/$Il2rg^{-/-}$ mice. When used as single agents, lapatinib and crizotinib inhibited tumor growth to a similar extent. Intriguingly, the inhibitory effect of the 2 inhibitors in combination was significantly larger (Figure 8A). We did not note any toxic effect of the combination of drugs, and the mice that received it maintained a relatively stable weight during the treatment course (Figure 8B). Immunoblotting of tumor lysates confirmed correct target inhibition under the various treatment regimens (Supplemental Figure 9).

To obtain insight into the antitumor effect of the combination of drugs, we conducted immunohistochemical studies on tumor sections. Interestingly, lapatinib and crizotinib inhibited tumor

Figure 7
The β4 integrin is often coexpressed with ErbB2 and c-Met in human prostate cancer. (**A**) TMA slides comprising adjacent sections from 35 prostate adenocarcinomas (TMA-35) were stained with the indicated antibodies. The graphs show the staining intensity generated by each antibody across all samples. The concordance of staining intensity between the 2 anti-β4 mAbs and the coexpression of β4 with ErbB2 and c-Met were validated by the χ^2 test. (**B**) Serial sections of a primary prostate cancer (carcinoma) and adjacent normal glands (N) were subjected to immunohistochemistry with the indicated antibodies, followed by counterstaining with hematoxylin. Scale bar: 50 μm.

cell proliferation to a similar extent, either as single agents or in combination (Figure 8C). In contrast, the combination of the 2 drugs induced tumor cell apoptosis and inhibited tumor angiogenesis to a significantly larger extent as compared with each drug when used as single agent (Figure 8, D and E). Taken together, these results suggest that combined inhibition of ErbB2 and c-Met may display therapeutic efficacy in the relatively large fraction of prostate cancers that express elevated levels of the 2 RTKs.

Discussion

We have used an integrated approach, combining analysis of mouse models, genetic manipulation of human cancer cell lines, and molecular pathology to dissect the role of the β4 integrin in prostate cancer. Our results provide evidence that the β4 integrin promotes prostate tumorigenesis by enhancing the self-renewal capacity of putative cancer stem cells and the prolifera-

tive ability of their immediate progeny, the transit-amplifying cells. Furthermore, mechanistic studies have revealed that β4 promotes the expansion of both types of prostate tumor progenitor cells by buttressing ErbB2 and c-Met signaling. These results suggest that prostate progenitor cells remain dependent on niche signals that presumably operate, although in a redundant fashion, in their normal counterpart. In addition, they identify a form of non-oncogene dependency that should be amenable to pharmacological inhibition.

Many adult stem cells reside in niches spatially organized by a basement membrane (19), raising the possibility that laminin-binding integrins regulate their behavior. In agreement with this hypothesis, inactivation of multiple β1 integrins, which also comprise various laminin receptors, causes defects in the orientation of the basal cell division axis and impairs the regenerative potential of skin and mammary epithelium (70–72). Furthermore, genetic
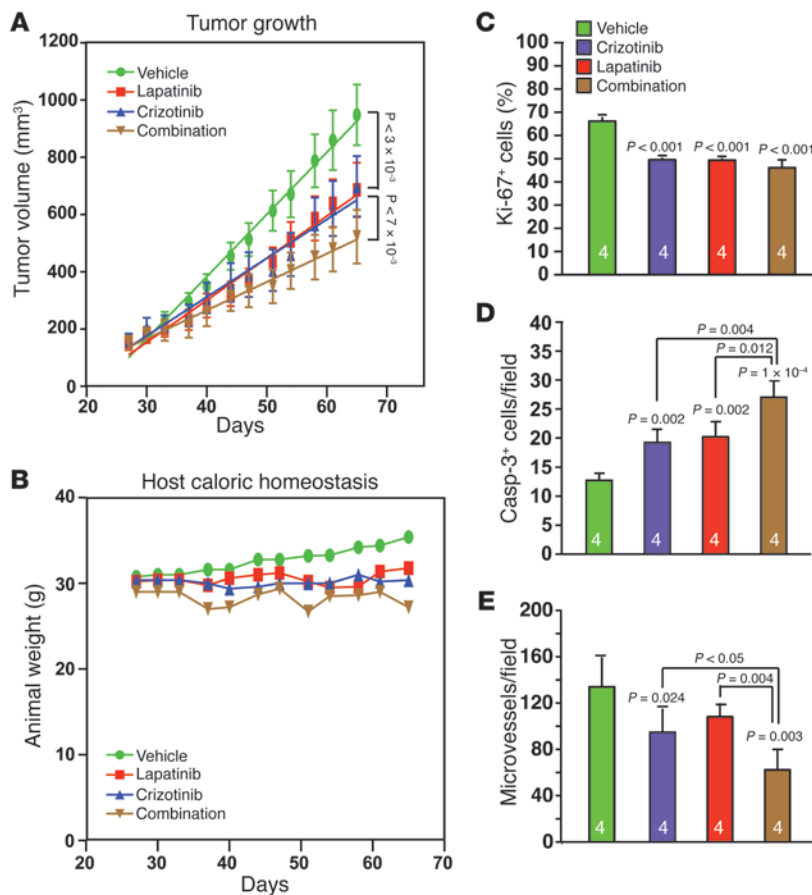
Figure 8
Simultaneous pharmacological inhibition of ErbB2 and c-Met inhibits prostate cancer growth in vivo. (**A**) 5×10^6 DU1455 cells were injected subcutaneously together with Matrigel in 8-week-old NOD/SCID/*Il2rg*$^{-/-}$ mice. Once tumors reached approximately 200 mm³, mice were randomized to receive lapatinib alone, crizotinib alone, lapatinib and crizotinib in combination, or vehicle control. The following doses were given: 150 mg/kg lapatinib p.o. daily for 5 days per week for 3 weeks and 50 mg/kg crizotinib p.o. daily for 5 days per week for 3 weeks. The graph shows the mean (± SD) tumor size at the indicated times. (**B**) The mean weight of mice treated as indicated at the indicated times. (**C**) Tumor sections were stained with anti–Ki-67. The graph shows the mean (± SD) percentage of Ki-67⁺ tumor cells in the indicated treatment groups. (**D**) Tumor sections were stained with anti–cleaved caspase-3 (Casp-3). The graph shows the mean (± SD) percentage of apoptotic tumor cells in the indicated treatment groups. (**E**) Tumor sections were stained with anti–PECAM-1. The graph shows the mean (± SD) number of microvessels per microscopic field in the indicated treatment groups. Numbers in columns represent the number of mice.

experiments have suggested that focal adhesion kinase, which is activated by multiple β1 integrins, promotes the expansion of tumor progenitor cells in mouse models of mammary and intestinal tumorigenesis (73–75). Finally, although not directly focusing on tumor progenitor cells, prior studies have emphasized a role for β1 integrins, but not for β4, in prostate cancer (37, 76–79). Our observation that β4 signaling is dispensable for prostate development but not tumorigenesis is consistent with the hypothesis that tumor cells are exquisitely dependent on certain integrin signaling pathways, such as those activated by β4, whereas their normal counterpart are not (32, 74).

Motivated by the prior observation that the expression of β4 is restricted to the basal compartment of the normal prostate and our finding that a subset of seemingly aggressive human prostate cancers overexpresses the β4 integrin, we introduced a targeted deletion of the β4 signaling domain in PB-*TAg* mice. We found that loss of β4 signaling inhibits tumor growth and delays progression to metastasis in these mice. Intriguingly, deletion of the β4 signaling domain impaired the ability of prostate tumor progenitors to form tumor spheres in vitro and to proliferate in vivo. Moreover, tissue recombination experiments revealed that prostate epithelial-specific deletion of the β4 signaling domain suppresses oncogenesis driven by loss of *Pten*, a common lesion in human prostate cancer. These findings suggest that integrin β4 signaling sustains both self-renewal and rapid proliferation of tumor progenitors in vivo. Moreover, since the expression of β4 is restricted to the fraction of tumor cells attached to the basement

membrane, our results support the model that prostate tumors contain a basal compartment consisting of putative stem cells able to undergo self-renewal as well as transit-amplifying cells undergoing rapid proliferation. In agreement with the hypothesis that integrin β4 signaling plays a unique role in prostate tumorigenesis, others have shown that genetic ablation of FAK does not impair tumor initiation or progression to adenocarcinoma in PB-*TAg* mice (80), suggesting that the β1 integrin/FAK signaling axis does not contribute to prostate tumorigenesis.

Biochemical studies revealed that the β4 integrin supports the expansion of prostate tumor progenitors in PB-*TAg* mice by buttressing activation of ErbB2 and c-Met and downstream signaling. Interestingly, we found that the putative tumor progenitor cells isolated from Hi-*Myc* and *Pten*$^{PC/PC}$ mice also expressed high levels of ErbB2/ErbB3 and c-Met, suggesting that these 2 tyrosine kinases sustain tumor progenitor cells independently of the oncogenic mutations that they possess. In agreement with this hypothesis, pharmacological inactivation of ErbB2/ErbB3 and c-Met inhibited the ability of tumor progenitor cells from all 3 mouse models to form prostatospheres in vitro. These results indicate that the β4 integrin promotes prostate tumorigenesis by buttressing mitogenic signaling in 2 distinct progenitor compartments across 3 mouse models of prostate tumorigenesis.

Prior studies have identified critical roles for ErbB2 and c-Met signaling in promoting progression of prostate cancer to androgen independence (49, 81–83). Since AR signaling suppresses the expression of β4, c-Met, and ErbB2 (84, 85), androgen withdrawal

may lead to a concordant upregulation of β4 and its partner RTKs, favoring the outgrowth of androgen-independent progenitor cells, which express β4 and the aforementioned RTKs. In agreement with this hypothesis, we found that primary prostate cancers treated with androgen ablation therapy exhibited elevated levels of *ITGB4* mRNA. Furthermore, we observed that the androgen-independent human prostate cancer DU145 and PC3 cells expressed high levels of β4, ErbB2, and c-Met, whereas the androgen-dependent LNCaP cells did not. Mechanistic studies indicated that silencing of β4 attenuates ErbB2 and c-Met signaling in DU145 cells and suppresses the ability of these cells to form subcutaneous tumors in nude mice. Conversely, ectopic expression of wild-type, but not mutant, β4 caused transactivation of ErbB2 and thereby tyrosine phosphorylation of the β4 signaling domain in LNCaP cells, enhancing subcutaneous growth in nude mice. These results indicate that β4 integrin promotes the oncogenic behavior of human prostate cancer cells by amplifying RTK signaling, in agreement with the results of our genetic analysis in mice.

Although a prior pathological study of low Gleason grade prostate cancer suggested that the β4 integrin is downregulated (37), COPA identified *ITGB4* as markedly overexpressed in a subset of tumor samples in 11 out of 16 available DNA microarray data sets. Interestingly, high-level expression of *ITGB4* was associated with high Gleason grade in primary tumors as well as with androgen-independent metastases to bone. In addition, immunohistochemistry on paraffin-embedded sections indicated that the neoplastic cells in virtually all PIN lesions and a significant fraction of invasive prostate cancers expressed the β4 integrin, often in combination with c-Met and ErbB2. Since the phenotype of human prostate cancer stem cells is incompletely defined, we were not able to examine whether these cells coexpress the β4 integrin, ErbB2, and c-Met. Nevertheless, our studies strongly suggest that the β4 integrin can sustain ErbB2 and c-Met signaling in human prostate cancer.

ErbB2 and c-Met appear to be activated in a fraction of human prostate cancers, either because of overexpression or in response to a paracrine signaling loop (49, 86, 87). Our results indicate that the β4 integrin is required for efficient activation of both RTKs and for downstream mitogenic signaling in both cancer stem cells and transit-amplifying cells. In addition, we found that the ErbB2 inhibitor lapatinib and the c-Met inhibitor crizotinib cooperate to suppress prostate cancer growth in the DU145 xenograft model. These results raise the possibility that these or similar agents may display therapeutic efficacy in castration-resistant prostate cancer, or even in the androgen-dependent phase of the disease, in combination with drugs targeting the AR.

Methods

Mouse strains. PB-*TAg*, Hi-*Myc* (ARR2-Pb-*cMyc*), and *Pten^{PC/PC}* (PB-Cre4; *Pten^{fl/fl}*) mice were previously described (50, 51). To generate control and β4 mutant PB-*TAg* mice, cohorts of PB-*TAg*; β4-1355T/WT littermates were intercrossed to yield PB-*TAg*; β4-1355T and PB-*TAg*; β4-WT mice. Mice were genotyped by PCR as previously described (39). All experiments were conducted in compliance with MSKCC IACUC guidelines. Wild-type C57BL/6J mice and NOD/SCID/*Il2rg^{-/-}* mice were purchased from The Jackson Laboratory. Timed-pregnant Sprague Dawley rats were purchased from Taconic.

Prostate cell preparation and sorting. The anterior lobe of the prostate was collected from mice at the indicated age, minced into small fragments, washed once in DMEM containing 0.5 mM EDTA, and digested with Accutase (Innovative Cell Technology) for 2 hours at 37°C. The cell suspension was passed through a 40-μm cell strainer. Dissociated prostate cells were suspended in PBS with 10% FBS and stained with the indicated antibody for 30 minutes at 4°C. Dead cells were sorted out by staining with DAPI. Cell sorting was done using the BD FACSAria II.

FACS analysis and EdU incorporation. Cell surface expression was performed using the Dako CyAN flow cytometer, followed by analysis with FlowJo software. For EdU labeling of mouse prostate, 25 μg/g/d EdU was injected intraperitoneally for the indicated time. Tissue was harvested as described above, and samples were depleted of Lin^+ cells using magnetic beads coated with antibodies against CD31 (MEC 13.3, BD Pharmingen) and CD45 (30-F11, BD Pharmingen) and then stained with the LIVE/DEAD Fixable Dead Cell Staining Kit (Invitrogen) prior to fixation. EdU staining was subsequently performed using the Click-iT Edu Flow Cytometry Assay Kit (Invitrogen).

Sphere-forming assay and immunocytochemistry. The sphere-forming assay was performed following the conditions previously described (12). The different cell subpopulations were sorted by FACS, diluted to a concentration of 30,000 cells in 1.5 ml of prostatosphere medium (DMEM with high glucose, 2 mM L-glutamine, penicillin-streptomycin-fluconazole, supplement B27 [Gibco], 20 ng/ml EGF, 20 ng/ml bFGF, 4 μg/ml heparin, 5 μg/ml insulin, 0.5 μg/ml hydrocortisone), and seeded in triplicate in 24-well ultra-low-attachment plates (Costar). After 12 days, spheres were counted, and live cells were counted following trypan blue staining.

To assay for sphere-forming capability in the presence of RTK inhibitors, DP cells from 4.5-month-old PB-*TAg*; β4-WT mice were sorted and cultured as described above and treated with DMSO alone, 100 nM PHA665752 (S1070, Selleck), 100 nM lapatinib (S1028, Selleck), or a combination of both inhibitors.

Tumor allografts. For subrenal prostate regeneration assay, whole prostates were digested successively with a mix of Collagenase/Hyaluronidase (07912, StemCell Technologies) in 5% FBS DMEM/F12, then with 0.25% Trypsin/EDTA all in a cold room for 1 hour, and finally with prewarmed Dispase (07913, StemCell Technologies) with Dnase. The cell suspension was strained with a 40-μm filter, and 300,000 of total cells were spin infected with 1.25×10^7 PFUs of the respective lentivirus (Sigma-Aldrich). After that step, 250,000 rat UGM cells freshly isolated from E18 rat embryos were added to the cell suspension, pelleted, resuspended in 10 μl of Collagen I (BD 354249), plated in 6-well dishes to allow the collagen recomb graft to solidify, and, lastly, incubated overnight in DMEM 10% FBS 100 nM DHT. The following morning anesthetized NOD/SCID/*Il2rg^{-/-}* mice were used to implant the recomb plugs underneath the renal capsule. The kidneys were harvested at 12 weeks after surgery.

For orthotopic implantation of tumors of PB-*TAg* mice, 50,000 sorted cells from each population of PB-*TAg*; β4-WT and PB-*TAg*; β4-1355T mice were resuspended in Matrigel diluted 1:1 in PrENC medium (Lonza) and injected in the right anterior prostatic lobe of NOD/SCID/*Il2rg^{-/-}* mice. These mice were also implanted with 90-day release testosterone pellets (12.5 mg/pellet; Innovative Research of America). 90 days after implantation, mice were euthanized, and prostate lobes were dissected and fixed in 4% paraformaldehyde, mounted in paraffin, sectioned, and subjected to immunohistochemistry.

RNA extraction and RT-PCR. RNA was extracted from sorted cells using the RNAqueous-Micro Scale RNA Isolation Kit (Ambion). RT-PCR was performed using the SuperScript III One Step RT-PCR System (Invitrogen).

Mouse pathology. Pathological examination and histological classification of the tumors were performed according to previous guidelines (42, 88). To examine histological progression, we estimated the percentage of each prostate sample containing hyperplasia, low-grade PIN, high-grade PIN, well-differentiated and moderately differentiated carcinoma, and poorly

differentiated carcinoma at the indicated time points. These tissues and xenografts were embedded in paraffin or snap frozen in OCT compound. Paraffin-embedded or frozen sections were subjected to immunoperoxidase staining with mouse mAb to Ki-67 (NCC-Ki-67-MM1, Novocastra), rabbit antibody to AR (PG-21, Upstate Biotechnology) performed with the ABC or MOM Kit (Vector Laboratories), and immunofluorescent staining on fresh frozen sections with rat mAb to β4 (346-11A, BD Biosciences), to PECAM-1 (MEC 13.3, BD Biosciences), and to E-cadherin (ECCD-2, Zymed) as well as rabbit antibody to keratin 14 (MK 14, Babco), to ErbB2 (Cell Signaling), to p-Akt (Ser473, Cell Signaling), to Met (C-28, Santa Cruz Biotechnology), and to the LE4-6 modules of the mouse laminin γ2 chain (89), with FITC- and Cy3-conjugated (both from Jackson Immuno-Research Laboratories) and Alexa Fluor 488– and Alexa Fluor 594–conjugated (both from Invitrogen) secondary antibodies.

MRI analysis. Mice were anesthetized with isoflurane. Images were obtained on a 1.5-T General Electric Horizon Signa Scanner (General Electric Medical Systems) using a homemade foil solenoid coil with a 27-mm inner diameter. After obtaining low-resolution sagittal and axial images, high spatial resolution axial imaging using a fast spin echo sequence (repetition interval = 2,000–3,000 ms, effective echo time = 102 ms, 12 echoes per phase encoding step, spatial resolution = 1.5-mm slice thickness, 156 × 156 mm or 156 × 208 mm in plane resolution, and 6 to 12 repetitions, 6–8 minutes of data acquisition) was performed. Tumor volumes were estimated from the sum of the pixels occupied by the enlarged prostate in each of the slices and the interval between slices. Normal mice were examined in parallel to obtain the volume of the normal prostate.

Human pathology. We analyzed an existing DNA microarray data set as previously described (90). Values for the probes to either β4 or α6 were averaged. LNCaP cells grown in the presence of androgen were used as a negative control for the expression of β4. Tissue arrays containing 104 paraffin-embedded sections from primary prostate cancer (MSKCC tissue collection) as well other commercially available arrays containing 35 and 39 paraffin-embedded sections from primary prostate cancer and metastasis (Biomax) were deparaffinized in a descending ethanol series, quenched with 3% H_2O_2, digested with 0.1% pepsin at room temperature for 10 minutes, subjected to steam antigen retrieval or with Target Retrival Solution (DAKO) for 40 minutes, and then stained with the mouse mAb to β4 (ELF1, Novocastra), rat mAb to β4 (439-9B, BD Biosciences), rabbit pAb to ErbB2 (DAKO) and to Met (C-28, Santa Cruz Biotechnology), and mouse mAb to CD44 (R&D Systems) using the ABC Staining Kit (Vector Laboratories) or LSAB Staining Kit (DAKO).

DNA transfection and RNA interference. LNCaP cells were transfected with vectors encoding human β4-WT or β4-1355T (25) using Lipofectamine 2000 (Invitrogen). Stable transfectants were selected with 500 μg/ml G418 (Gibco). DU145 cells were transduced with a retrovirus (LTRHI-hygro) directing the expression of a shRNA to β4 (targeting GAGCUGCACG-GAGUGUGUC) or a control shRNA (targeting AGCCACACACTTGTG-GAAC) and selected with 30 μg/ml Hygromycin (Calbiochem) or a lentivirus directing the expression of a shRNA against β4 or a nontargeting control and selected with puromycin 3 μg/ml (clone TRCN0000057768 and TRCN0000057771, Open Biosystem).

Cell biology studies and tumor xenografts. To measure cell proliferation in vitro, cells were deprived of growth factors and then incubated in medium containing 1% FBS and BrdU with or without 50 ng/ml NRG for 14 hours. Then, they were subjected to immunofluorescent staining with anti-BrdU antibody using the BrdU Labeling and Detection Kit I (Roche). To estimate invasive ability in vitro, cells were deprived of serum and growth factors for 24 hours, after which 1 × 10⁵ cells were seeded, placed in the upper chamber of Cell Culture Inserts (Becton Dickinson; 8-mm pores), and coated with 70 μl of 1 mg/ml Matrigel (BD Biosciences). After 24 hours, inserts

were fixed with 4% paraformaldehyde for 10 minutes at room temperature and stained with 0.5% crystal violet.

To measure cell proliferation in vivo, cryostat sections of prostate tumors or xenografts were subjected to immunohistochemical staining with anti–Ki-67 antibody. To estimate cell death in vivo, TUNEL assays were performed on frozen sections (In Situ Cell Death Detection Kit; Roche). Intraductal microvessel density was estimated as previously described (44).

To make tumor xenografts, 5 × 10⁶ LNCaP transfectants and 2 × 10⁶ DU145 derivatives were resuspended in Matrigel diluted 1:1 in PBS and injected subcutaneously in the flanks of 6- to 8-week-old male athymic nude mice. The tumors generated by LNCaP transfectants were excised 17 days after implantation, and those formed by DU145 derivatives were excised 32 days after implantation. Tumors were weighed and then subjected to H&E staining and immunohistochemical analysis.

To examine the preclinical efficacy of combined pharmacological inhibition of HER2 and c-Met, 8-week-old NOD/SCID male mice (Taconic) were injected subcutaneously with 5 × 10⁶ DU1455 cells together with Matrigel (BD Biosciences). Once tumors reached approximately 200 mm³, mice were randomized to receive lapatinib alone, crizotinib alone, lapatinib and crizotinib in combination, or vehicle control. Dosing schedule was as follows: 150 mg/kg lapatinib p.o. daily 5 times for 3 weeks; 50 mg/kg crizotinib p.o. daily 5 times for 3 weeks. Tumor size was measured twice weekly by caliper in control and treatment groups, and the average tumor volume in each group was expressed in cubic millimeter and calculated using the following formula: π/6 × (large diameter) × (small diameter)². At the end of treatment, a subset of tumors was dissected and cut in half, and one part was frozen in liquid nitrogen to be used in biochemical studies and one part was processed for immunohistochemical analysis.

Biochemical studies. Primary β4-positive cells from PB-*TAg*; β4-WT or PB-*TAg*; β41355T tumors were sorted by FACS, plated onto laminin-coated plates, starved for 6 hours, and then treated with 50 ng/ml NRG1 (R&D Systems), 50 ng/ml HGF (Biosource), or maintained in starvation. Cells were lysed in SDS buffer with protease and phosphatase inhibitors. Human prostate cell lines were lysed in 10 mM Tris, pH 7.6, 50 mM NaCl, 1% NP40, 10% glycerol with protease, and phosphatase inhibitors and subjected to immunoprecipitation and immunoblotting analyses.

Other antibodies and reagents. Goat antibody to β4 (C-20), rabbit antibodies to β4 (H101), EGFR (1005), Met (C-28), ErbB2 (C-18), and mouse mAb to Shc (pG-797) were from Santa Cruz Biotechnology. Rabbit antibodies to ErbB2, P-ERK1/2, P-AKT (Ser473), P-JNK, and P-Shc (Tyr317) were from Cell Signaling Technology. Mouse mAbs to Vinculin (clone hVIN-1) and Actin (clone AC-40) were from Sigma-Aldrich. Rat mAbs to P-Tyr (RC-20) and mouse mAb to SV40 LT (clone Pab101) were from BD Biosciences. Affinity-purified mouse mAb 3E1 to β4 was described previously (91). PE anti–integrin β4 antibody (clone 346-11A, Abcam), PerCP/Cy5.5 anti–Sca-1 (clone D7, BioLegend), Alexa Fluor 488 anti-CD44 (clone IM7, BioLegend), and anti–TROP-2 (AF650, R&D Systems) were also used. Biotinylated secondary antibodies were from Vector Laboratories, and HRP-conjugated secondary antibodies were from Santa Cruz Biotechnology. Laminin-5 matrices were prepared as previously described (92). Human fibronectin (BD Biosciences) and recombinant human NRG-1-β1 and HGF were from R&D Systems. Pepsin and DAB were from Sigma-Aldrich.

Statistics. For Kaplan-Meier analysis of survival, statistical significance was determined by the log-rank test. Two-tailed Student's or Welch *t* test, χ^2 test, and 2-way ANOVA tests were otherwise used to determine statistical significance between experimental groups.

Study approval. All animal studies received prior approval by the IACUC of MSKCC and were conducted in compliance with its recommendations. All human studies were reviewed and approved by the IRB of MSKCC, and written informed consent was provided for human samples.

1. Isaacs W, De Marzo A, Nelson WG. Focus on prostate cancer. *Cancer Cell*. 2002;2(2):113–116.
2. Scher HI, Sawyers CL. Biology of progressive, castration-resistant prostate cancer: directed therapies targeting the androgen-receptor signaling axis. *J Clin Oncol*. 2005;23(32):8253–8261.
3. Shen MM, Abate-Shen C. Molecular genetics of prostate cancer: new prospects for old challenges. *Genes Dev*. 2010;24(18):1967–2000.
4. Kumar-Sinha C, Tomlins SA, Chinnaiyan AM. Recurrent gene fusions in prostate cancer. *Nat Rev Cancer*. 2008;8(7):497–511.
5. Taylor BS, et al. Integrative genomic profiling of human prostate cancer. *Cancer Cell*. 2010;18(1):11–22.
6. Clevers H. The cancer stem cell: premises, promises and challenges. *Nat Med*. 2011;17(3):313–319.
7. Gupta PB, Chaffer CL, Weinberg RA. Cancer stem cells: mirage or reality? *Nat Med*. 2009; 15(9):1010–1012.
8. Shackleton M, Quintana E, Fearon ER, Morrison SJ. Heterogeneity in cancer: cancer stem cells versus clonal evolution. *Cell*. 2009;138(5):822–829.
9. Sawyers C. Targeted cancer therapy. *Nature*. 2004; 432(7015):294–297.
10. Cunha GR, et al. The endocrinology and developmental biology of the prostate. *Endocr Rev*. 1987; 8(3):338–362.
11. Lawson DA, Xin L, Lukacs RU, Cheng D, Witte ON. Isolation and functional characterization of murine prostate stem cells. *Proc Natl Acad Sci U S A*. 2007;104(1):181–186.
12. Wang X, et al. A luminal epithelial stem cell that is a cell of origin for prostate cancer. *Nature*. 2009; 461(7263):495–500.
13. Foster CS, Dodson A, Karavana V, Smith PH, Ke Y. Prostatic stem cells. *J Pathol*. 2002;197(4):551–565.
14. Okada H, et al. Keratin profiles in normal/hyperplastic prostates and prostate carcinoma. *Virchows Arch A Pathol Anat Histopathol*. 1992;421(2):157–161.
15. Choi N, Zhang B, Zhang L, Ittmann M, Xin L. Adult murine prostate basal and luminal cells are self-sustained lineages that can both serve as targets for prostate cancer initiation. *Cancer Cell*. 2012; 21(2):253–265.
16. Goldstein AS, Huang J, Guo C, Garraway IP, Witte ON. Identification of a cell of origin for human prostate cancer. *Science*. 2010;329(5991):568–571.
17. Lawson DA, Zong Y, Memarzadeh S, Xin L, Huang J, Witte ON. Basal epithelial stem cells are efficient targets for prostate cancer initiation. *Proc Natl Acad Sci U S A*. 2010;107(6):2610–2615.
18. Borovski T, De Sousa EMF, Vermeulen L, Medema JP. Cancer stem cell niche: the place to be. *Cancer Res*. 2011;71(3):634–639.
19. Morrison SJ, Spradling AC. Stem cells and niches: mechanisms that promote stem cell maintenance throughout life. *Cell*. 2008;132(4):598–611.
20. Visvader JE. Keeping abreast of the mammary epithelial hierarchy and breast tumorigenesis. *Genes Dev*. 2009;23(22):2563–2577.
21. Lathia JD, et al. Integrin alpha 6 regulates glioblastoma stem cells. *Cell Stem Cell*. 2010;6(5):421–432.
22. Hao J, Yang Y, McDaniel KM, Dalkin BL, Cress AE, Nagle RB. Differential expression of laminin 5 (alpha 3 beta 3 gamma 2) by human malignant and normal prostate. *Am J Pathol*. 1996;149(4):1341–1349.
23. Giancotti FG, Ruoslahti E. Integrin signaling. *Science*. 1999;285(5430):1028–1032.
24. Guo W, Giancotti FG. Integrin signalling during tumour progression. *Nat Rev Mol Cell Biol*. 2004; 5(10):816–826.
25. Dans M, Gagnoux-Palacios L, Blaikie P, Klein S, Mariotti A, Giancotti FG. Tyrosine phosphorylation of the beta 4 integrin cytoplasmic domain mediates Shc signaling to extracellular signal-regulated kinase and antagonizes formation of hemidesmosomes. *J Biol Chem*. 2001;276(2):1494–1502.
26. Gagnoux-Palacios L, et al. Compartmentalization of integrin alpha6beta4 signaling in lipid rafts. *J Cell Biol*. 2003;162(7):1189–1196.
27. Mainiero F, et al. The coupling of alpha6beta4 integrin to Ras-MAP kinase pathways mediated by Shc controls keratinocyte proliferation. *EMBO J*. 1997;16(9):2365–2375.
28. Shaw LM, Rabinovitz I, Wang HH, Toker A, Mercurio AM. Activation of phosphoinositide 3-OH kinase by the alpha6beta4 integrin promotes carcinoma invasion. *Cell*. 1997;91(7):949–960.
29. Mariotti A, Kedeshian PA, Dans M, Curatola AM, Gagnoux-Palacios L, Giancotti FG. EGF-R signaling through Fyn kinase disrupts the function of integrin alpha6beta4 at hemidesmosomes: role in epithelial cell migration and carcinoma invasion. *J Cell Biol*. 2001;155(3):447–458.
30. Trusolino L, Bertotti A, Comoglio PM. A signaling adapter function for alpha6beta4 integrin in the control of HGF-dependent invasive growth. *Cell*. 2001;107(5):643–654.
31. Santoro MM, Gaudino G, Marchisio PC. The MSP receptor regulates alpha6beta4 and alpha3beta1 integrins via 14-3-3 proteins in keratinocyte migration. *Dev Cell*. 2003;5(2):257–271.
32. Guo W, et al. Beta 4 integrin amplifies ErbB2 signaling to promote mammary tumorigenesis. *Cell*. 2006;126(3):489–502.
33. Tomlins SA, et al. Recurrent fusion of TMPRSS2 and ETS transcription factor genes in prostate cancer. *Science*. 2005;310(5748):644–648.
34. LaTulippe E, et al. Comprehensive gene expression analysis of prostate cancer reveals distinct transcriptional programs associated with metastatic disease. *Cancer Res*. 2002;62(15):4499–4506.
35. Singh D, et al. Gene expression correlates of clinical prostate cancer behavior. *Cancer Cell*. 2002; 1(2):203–209.
36. Holzbeierlein J, et al. Gene expression analysis of human prostate carcinoma during hormonal therapy identifies androgen-responsive genes and mechanisms of therapy resistance. *Am J Pathol*. 2004; 164(1):217–227.
37. Davis TL, Cress AE, Dalkin BL, Nagle RB. Unique expression pattern of the alpha6beta4 integrin and laminin-5 in human prostate carcinoma. *Prostate*. 2001;46(3):240–248.
38. Gilcrease MZ, et al. Coexpression of alpha6beta4 integrin and guanine nucleotide exchange factor Net1 identifies node-positive breast cancer patients at high risk for distant metastasis. *Cancer Epidemiol Biomarkers Prev*. 2009;18(1):80–86.
39. Nikolopoulos SN, Blaikie P, Yoshioka T, Guo W, Giancotti FG. Integrin beta4 signaling promotes tumor angiogenesis. *Cancer Cell*. 2004;6(5):471–483.
40. Nikolopoulos SN, et al. Targeted deletion of the integrin beta4 signaling domain suppresses laminin-5-dependent nuclear entry of mitogen-activated protein kinases and NF-kappaB, causing defects in epidermal growth and migration. *Mol Cell Biol*. 2005;25(14):6090–6102.
41. Greenberg NM, et al. Prostate cancer in a transgenic mouse. *Proc Natl Acad Sci U S A*. 1995; 92(8):3439–3443.
42. Kaplan-Lefko PJ, et al. Pathobiology of autochthonous prostate cancer in a pre-clinical transgenic mouse model. *Prostate*. 2003;55(3):219–237.
43. Chiaverotti T, et al. Dissociation of epithelial and neuroendocrine carcinoma lineages in the transgenic adenocarcinoma of mouse prostate model of prostate cancer. *Am J Pathol*. 2008;172(1):236–246.
44. Huss WJ, Hanrahan CF, Barrios RJ, Simons JW, Greenberg NM. Angiogenesis and prostate cancer: identification of a molecular progression switch. *Cancer Res*. 2001;61(6):2736–2743.
45. Mulholland DJ, Xin L, Morim A, Lawson D, Witte O, Wu H. Lin-Sca-1+CD49fhigh stem/progenitors are tumor-initiating cells in the Pten-null prostate cancer model. *Cancer Res*. 2009;69(22):8555–8562.
46. Lukacs RU, Memarzadeh S, Wu H, Witte ON. Bmi-1 is a crucial regulator of prostate stem cell self-renewal and malignant transformation. *Cell Stem Cell*. 2010;7(6):682–693.
47. Giancotti FG. Targeting integrin beta4 for cancer and anti-angiogenic therapy. *Trends Pharmacol Sci*. 2007;28(10):506–511.
48. Chen Y, Sawyers CL, Scher HI. Targeting the androgen receptor pathway in prostate cancer. *Curr Opin Pharmacol*. 2008;8(4):440–448.
49. Knudsen BS, Edlund M. Prostate cancer and the met hepatocyte growth factor receptor. *Adv Cancer Res*. 2004;91:31–67.
50. Ellwood-Yen K, et al. Myc-driven murine prostate cancer shares molecular features with human prostate tumors. *Cancer Cell*. 2003;4(3):223–238.
51. Wang S, et al. Prostate-specific deletion of the murine Pten tumor suppressor gene leads to metastatic prostate cancer. *Cancer Cell*. 2003;4(3):209–221.
52. Grasso AW, Wen D, Miller CM, Rhim JS, Pretlow TG, Kung HJ. ErbB kinases and NDF signaling

in human prostate cancer cells. *Oncogene*. 1997; 15(22):2705–2716.

53. Garraway IP, et al. Human prostate sphere-forming cells represent a subset of basal epithelial cells capable of glandular regeneration in vivo. *Prostate*. 2010;70(5):491–501.

54. Sobel RE, Wang Y, Sadar MD. Molecular analysis and characterization of PrEC, commercially available prostate epithelial cells. *In Vitro Cell Dev Biol Anim*. 2006;42(1–2):33–39.

55. Liu C, et al. The microRNA miR-34a inhibits prostate cancer stem cells and metastasis by directly repressing CD44. *Nat Med*. 2011;17(2):211–215.

56. Hynes NE, Lane HA. ERBB receptors and cancer: the complexity of targeted inhibitors. *Nat Rev Cancer*. 2005;5(5):341–354.

57. Trusolino L, Bertotti A, Comoglio PM. MET signalling: principles and functions in development, organ regeneration and cancer. *Nat Rev Mol Cell Biol*. 2010;11(12):834–848.

58. Veeramani S, et al. Expression of p66(Shc) protein correlates with proliferation of human prostate cancer cells. *Oncogene*. 2005;24(48):7203–7212.

59. Vlietstra RJ, van Alewijk DC, Hermans KG, van Steenbrugge GJ, Trapman J. Frequent inactivation of PTEN in prostate cancer cell lines and xenografts. *Cancer Res*. 1998;58(13):2720–2723.

60. Sgambato A, et al. Targeted inhibition of the epidermal growth factor receptor-tyrosine kinase by ZD1839 ('Iressa') induces cell-cycle arrest and inhibits proliferation in prostate cancer cells. *J Cell Physiol*. 2004;201(1):97–105.

61. Wallace TA, et al. Tumor immunobiological differences in prostate cancer between African-American and European-American men. *Cancer Res*. 2008;68(3):927–936.

62. Glinsky GV, Glinskii AB, Stephenson AJ, Hoffman RM, Gerald WL. Gene expression profiling predicts clinical outcome of prostate cancer. *J Clin Invest*. 2004;113(6):913–923.

63. Vanaja DK, Cheville JC, Iturria SJ, Young CY. Transcriptional silencing of zinc finger protein 185 identified by expression profiling is associated with prostate cancer progression. *Cancer Res*. 2003; 63(14):3877–3882.

64. Ito M, et al. Stem cells in the hair follicle bulge contribute to wound repair but not to homeostasis of the epidermis. *Nat Med*. 2005;11(12):1351–1354.

65. Villadsen R, et al. Evidence for a stem cell hierarchy in the adult human breast. *J Cell Biol*. 2007; 177(1):87–101.

66. Collins AT, Berry PA, Hyde C, Stower MJ, Maitland NJ. Prospective identification of tumorigenic prostate cancer stem cells. *Cancer Res*. 2005; 65(23):10946–10951.

67. Patrawala L, et al. Highly purified CD44+ prostate cancer cells from xenograft human tumors are enriched in tumorigenic and metastatic progenitor cells. *Oncogene*. 2006;25(12):1696–1708.

68. Xia W, et al. Anti-tumor activity of GW572016: a dual tyrosine kinase inhibitor blocks EGF activation of EGFR/erbB2 and downstream Erk1/2 and

AKT pathways. *Oncogene*. 2002;21(41):6255–6263.

69. Cui JJ, et al. Structure based drug design of crizotinib (PF-02341066), a potent and selective dual inhibitor of mesenchymal-epithelial transition factor (c-MET) kinase and anaplastic lymphoma kinase (ALK). *J Med Chem*. 2011;54(18):6342–6363.

70. Raghavan S, Bauer C, Mundschau G, Li Q, Fuchs E. Conditional ablation of beta1 integrin in skin. Severe defects in epidermal proliferation, basement membrane formation, and hair follicle invagination. *J Cell Biol*. 2000;150(5):1149–1160.

71. Lechler T, Fuchs E. Asymmetric cell divisions promote stratification and differentiation of mammalian skin. *Nature*. 2005;437(7056):275–280.

72. Taddei I, et al. Beta1 integrin deletion from the basal compartment of the mammary epithelium affects stem cells. *Nat Cell Biol*. 2008;10(6):716–722.

73. Luo M, et al. Mammary epithelial-specific ablation of the focal adhesion kinase suppresses mammary tumorigenesis by affecting mammary cancer stem/progenitor cells. *Cancer Res*. 2009;69(2):466–474.

74. Pylayeva Y, Gillen KM, Gerald W, Beggs HE, Reichardt LF, Giancotti FG. Ras- and PI3K-dependent breast tumorigenesis in mice and humans requires focal adhesion kinase signaling. *J Clin Invest*. 2009; 119(2):252–266.

75. Ashton GH, et al. Focal adhesion kinase is required for intestinal regeneration and tumorigenesis downstream of Wnt/c-Myc signaling. *Dev Cell*. 2010; 19(2):259–269.

76. Fornaro M, Tallini G, Bofetiado CJ, Bosari S, Languino LR. Down-regulation of beta 1C integrin, an inhibitor of cell proliferation, in prostate carcinoma. *Am J Pathol*. 1996;149(3):765–773.

77. Goel HL, et al. beta1A integrin expression is required for type 1 insulin-like growth factor receptor mitogenic and transforming activities and localization to focal contacts. *Cancer Res*. 2005;65(15):6692–6700.

78. Goel HL, Underwood JM, Nickerson JA, Hsieh CC, Languino LR. Beta1 integrins mediate cell proliferation in three-dimensional cultures by regulating expression of the sonic hedgehog effector protein, GLI1. *J Cell Physiol*. 2010;224(1):210–217.

79. Lamb LE, Zarif JC, Miranti CK. The androgen receptor induces integrin alpha6beta1 to promote prostate tumor cell survival via NF-kappaB and Bcl-xL independently of PI3K signaling. *Cancer Res*. 2011;71(7):2739–2749.

80. Slack-Davis JK, Hershey ED, Theodorescu D, Frierson HF, Parsons JT. Differential requirement for focal adhesion kinase signaling in cancer progression in the transgenic adenocarcinoma of mouse prostate model. *Mol Cancer Ther*. 2009;8(8):2470–2477.

81. Agus DB, et al. Targeting ligand-activated ErbB2 signaling inhibits breast and prostate tumor growth. *Cancer Cell*. 2002;2(2):127–137.

82. Craft N, Shostak Y, Carey M, Sawyers CL. A mechanism for hormone-independent prostate cancer through modulation of androgen receptor signaling by the HER-2/neu tyrosine kinase. *Nat Med*. 1999;5(3):280–285.

83. Mellinghoff IK, Vivanco I, Kwon A, Tran C, Wong-

vipat J, Sawyers CL. HER2/neu kinase-dependent modulation of androgen receptor function through effects on DNA binding and stability. *Cancer Cell*. 2004;6(5):517–527.

84. Bonaccorsi L, et al. Androgen receptor expression in prostate carcinoma cells suppresses alpha6beta4 integrin-mediated invasive phenotype. *Endocrinology*. 2000;141(9):3172–3182.

85. Verras M, Lee J, Xue H, Li TH, Wang Y, Sun Z. The androgen receptor negatively regulates the expression of c-Met: implications for a novel mechanism of prostate cancer progression. *Cancer Res*. 2007; 67(3):967–975.

86. Osman I, et al. HER-2/neu (p185neu) protein expression in the natural or treated history of prostate cancer. *Clin Cancer Res*. 2001;7(9):2643–2647.

87. Signoretti S, et al. Her-2-neu expression and progression toward androgen independence in human prostate cancer. *J Natl Cancer Inst*. 2000;92(23):1918–1925.

88. Shappell SB, et al. Prostate pathology of genetically engineered mice: definitions and classification. The consensus report from the Bar Harbor meeting of the mouse models of human cancer consortium prostate pathology committee. *Cancer Res*. 2004;64(6):2270–2305.

89. Sasaki T, et al. Short arm region of laminin-5 gamma2 chain: structure, mechanism of processing and binding to heparin and proteins. *J Mol Biol*. 2001; 314(4):751–763.

90. Stephenson AJ, et al. Integration of gene expression profiling and clinical variables to predict prostate carcinoma recurrence after radical prostatectomy. *Cancer*. 2005;104(2):290–298.

91. Giancotti FG, Stepp MA, Suzuki S, Engvall E, Ruoslahti E. Proteolytic processing of endogenous and recombinant beta 4 integrin subunit. *J Cell Biol*. 1992;118(4):951–959.

92. Spinardi L, Einheber S, Cullen T, Milner TA, Giancotti FG. A recombinant tail-less integrin beta 4 subunit disrupts hemidesmosomes, but does not suppress alpha 6 beta 4-mediated cell adhesion to laminins. *J Cell Biol*. 1995;129(2):473–487.

93. Welsh JB, et al. Analysis of gene expression identifies candidate markers and pharmacological targets in prostate cancer. *Cancer Res*. 2001; 61(16):5974–5978.

94. Magee JA, et al. Expression profiling reveals hepsin overexpression in prostate cancer. *Cancer Res*. 2001;61(15):5692–5696.

95. Luo JH, et al. Gene expression analysis of prostate cancers. *Mol Carcinog*. 2002;33(1):25–35.

96. Nanni S, et al. Epithelial-restricted gene profile of primary cultures from human prostate tumors: a molecular approach to predict clinical behavior of prostate cancer. *Mol Cancer Res*. 2006;4(2):79–92.

97. Varambally S, et al. Integrative genomic and proteomic analysis of prostate cancer reveals signatures of metastatic progression. *Cancer Cell*. 2005; 8(5):393–406.

98. True L, et al. A molecular correlate to the Gleason grading system for prostate adenocarcinoma. *Proc Natl Acad Sci U S A*. 2006;103(29):10991–10996.